JOURNAL OF CRIS



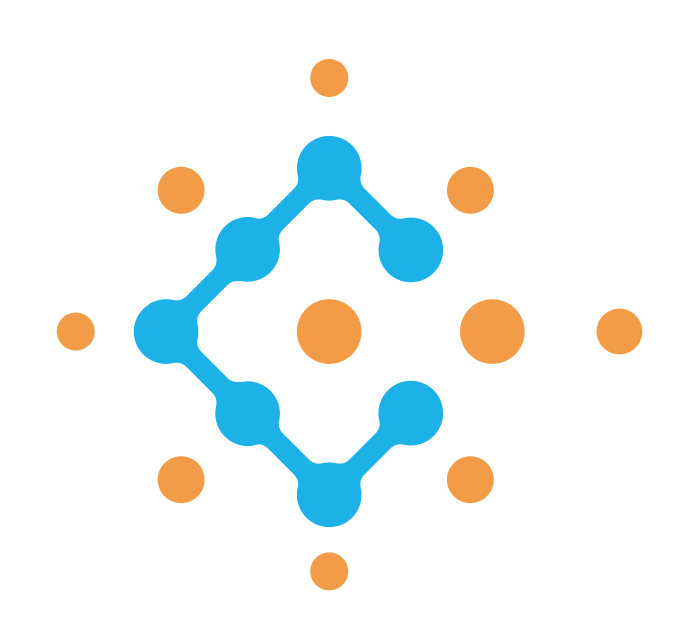


Table of **Contents**

02	Board Message	
03	Letter from the Editor	
04	Comparative Analysis of PVT Densities for Carbon Dioxide: Evaluating a New Equation of State Against Experimental Data and SRK Model Nida Tasneem and Shakeel Ahmed	
07	Synthesis of Aluminum Modified Sulfonated Activated Carbon for Phenol Removal from Water Faisal M. Alissa, Abdullah A. Alzahrani, Abdualilah I. Albaiz, and Saroj K. Panda	∠ a
19	Determination of Aliphatic Amines in Industrial Waste Water Using SPME Talal M. Al-Ghamdi	C
26	Green Catalytic Oxidation of Ethanol to Acetaldehyde Using Mentha spicata and Thymus vulgaris Extracts: A Sustainable Alternative to Metal Catalysts Saad Althubyani	
29	Novel Flash System for Determining Gas-Water Ratio in Reservoir Fluids Ahmed Sahl, Abdullah Almousa, Mohammed Bashrawi, and Faisal Alissa	
33	A Lab-Based Case Study of Root Cause Analysis of Filter Sludge Deposits from Natural Gas Liquid Recovery Plants and Quantitative Phase Analysis by Rietveld Method Muthukumar Nagu, Husin Sitepu, Wala A. Algozeeb, and Nayef M Alanazi	
47	Editorial Board	
48	Success Partners	

Board **Message**

Dear Esteemed Readers,

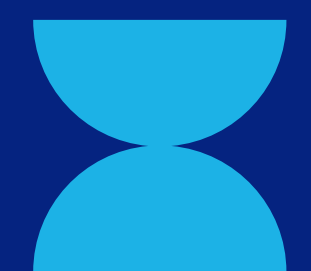
It is with immense pride and excitement that I welcome you to the first issue of volume 2 of our society's technical journal. Building on the foundation laid in our inaugural issue, this edition signifies our unwavering commitment to fostering innovation, sharing knowledge, and strengthening connections within our professional community.

As our field continues to evolve, so too does the scope of ideas and challenges we face. This journal remains dedicated to providing a platform where groundbreaking research, practical insights, and diverse perspectives converge. It is our hope that these contributions spark dialogue, inspire action, and drive meaningful progress.

In this issue, you will find an enriched selection of articles that delve deeper into the complexities of our discipline. Each piece reflects the dedication and expertise of our contributors, as well as the collective vision of our society to lead and inspire. I encourage you to explore the content thoughtfully and consider how these insights might shape your work and broaden your understanding.

The success of this endeavor would not be possible without the support and collaboration of our authors, reviewers, and editorial team. Their hard work and passion have once again made this journal a testament to the vibrancy and depth of our community. As we move forward, let us continue to celebrate the spirit of curiosity, innovation, and excellence that unites us. Thank you for your ongoing engagement and support. Together, we are shaping the future of our field.

Warm regards,





Letter From The Editor

Dear Colleagues,

Welcome to the first issue of Volume 2 of the Journal of Chemicals Research and Innovation Society. As we embark on another year of scientific exploration and knowledge sharing, we are excited to continue our mission of fostering groundbreaking research and collaboration in the chemical sciences.

Building on the foundation laid in our previous volumes, this issue presents a diverse collection of studies that showcase innovative methodologies, novel discoveries, and practical advancements across various fields of chemistry. Each contribution reflects the dedication and expertise of our research community, and we are proud to provide a platform for such impactful work.

I extend my deepest gratitude to our authors, reviewers, and editorial team for their unwavering commitment to excellence. Your contributions ensure that this journal remains a trusted source of scientific progress and a hub for meaningful discourse.

As we move forward, I encourage you to actively engage with the journal—whether through submitting your research, participating in discussions, or sharing insights with your peers. Together, we can continue to drive innovation and push the boundaries of chemical research.

Thank you for your continued support, and I look forward to the discoveries and advancements that lie ahead.

Best regards,

Shakeel Ahmed, Ph.D.,

Editor-in-Chief

Journal of Chemicals Research and Innovation Society

Comparative Analysis of PVT Densities for Carbon Dioxide: Evaluating a New Equation of State Against Experimental Data and SRK Model

Nida Tasneem¹ and Shakeel Ahmed ^{2,*}

¹Chemical Engineering Department,

²Interdisciplinary Research Center for Refining & Advanced Chemicals,
King Fahd University of Petroleum & Minerals, Dhahran, Saudi Arabia

*Corresponding author; email: shakeel@kfupm.edu.sa

Abstarct

This study compares the performance of a recently created equation of state (EOS) for carbon dioxide (CO2) against the Soave-Redlich-Kwong (SRK) equation and experimental data in order to predict PVT densities at different pressures and temperatures. The study highlights the new EOS's potential to improve CO2 control in industrial and environmental applications by demonstrating its higher accuracy, especially under high pressure.

Introduction

To maximize its use in industry and the environment, carbon dioxide (CO₂) must have its physical qualities accurately predicted under a range of pressures and temperatures (Mohagheghian et al., 2015). In order to enhance the accuracy of CO₂ density estimates, this work presents an enhanced equation of state (EOS). The research compares the prediction accuracy of the new EOS(Sterner & Pitzer, 1994) with the widely established Soave-Redlich-Kwong (SRK) equation using experimental data(Holland & Powell. 1991) theoretical formulations. In order to provide

insights into the performance of the new EOS at high pressures, where precise data is crucial for engineering applications, this comparison mainly focuses on measurement and analysis of densities at various temperature and pressure ranges(Herrig et al., 2018). This method advances our knowledge of how CO2 behaves in harsh environments and aids in the creation of more effective solutions for industries like environmental management and petrochemicals.

PVT comparison with experimental data and SRK Equation of State

1. Densities at different values of Temperature and Pressure

Densities of carbon dioxide are calculated using Equation of state that is described in the paper (Sterner & Pitzer, 1994) at different values of Temperature and different range of pressure. This equation of state has ability to generate accurate results even at very high pressure. In this equation of state, units used for pressure is kbar and for density is mol/cm³. Here are the values of constants for carbon dioxide.

Table 1. Constants for carbon dioxide

Term	Value	Units
Critical Pressure	0.073748	kbar
Critical Temperature	304.127	K
Critical Density	0.01063	mol/cm ³
Universal Gas Constant	0.083144626181 5324	(cm³.kbar)/(mol.K)
Acentric Factor	0.225	No unit

Pressure is held constant for calculation of density at different ranges of temperature. Pressure is held constant at 0.005 bar. Temperature range varied from 250 to 290 K. The densities are generated using MATLAB software and comparison with experimental data is displayed in tables below.

Table 2. Comparison of densities at different temperature from Experimental data

Temperature	Density (Experimental) (cm³/mol)	Density (EOS) (cm³/mol)	Absolute Error
250	0.00025216	0.0002522	4E-08
255	0.00024643	0.0002465	7E-08
260	0.00024099	0.000241	1E-08
265	0.00023581	0.0002358	1E-08
270	0.00023089	0.0002309	1E-08
275	0.00022619	0.0002262	1E-08
280	0.0002217	0.0002217	0
285	0.0002174	0.0002173	1E-07
290	0.00021328	0.0002132	8E-08
	3.66667E-08		

This equation of state almost gives same value of densities as that of experimental values taken from NIST. The mean absolute error is also very low that indicates the reliability of this equation of state. In a similar way, there is comparison of Pressure and densities by keeping temperature constant at 250K.

Table 3. Comparison of densities at different Pressure from Experimental data

Pressure (Kbar)	Density (Experimental) (cm³/mol)	Density (EOS) (cm³/mol)	Absolute Error		
0.001	0.0004852	0.000485	2E-07		
0.002	0.0009797	0.00098	3E-07		
0.003	0.0001739	0.0001484	0.0000255		
0.004	0.00019973	0.0001998	7E-08		
0.005	0.00025216	0.0002522	4E-08		
	Mean absolute error				

2. Comparison of Densities with SRK Model

Soave-Redlick-Kwong Equation of state is another EOS for calculation of PVT data of pure components. It is very common EOS that is used in different areas of petroleum and chemical engineering. Densities of carbon dioxide are also measured at different values of temperature from SRK and are compared with EOS of the paper. The results given below are comparable.

Table 4. Comparison of SRK Model with EOS using densities

Temperature	Density (Experimental) (cm³/mol)	Density (EOS) (cm³/mol)	Absolute Error
250	0.00025217	0.0002522	3E-08
255	0.000246	0.0002465	5E-07
260	0.0002407	0.000241	3E-07
265	0.0002356	0.0002358	2E-07
270	0.0002307	0.0002309	2E-07
275	0.0002261	0.0002262	1E-07
280	0.0002216	0.0002217	1E-07
285	0.0002173	0.0002173	0
290	0.0002132	0.0002132	0
	1.58889E-07		

The mean absolute error is very small. It means that the two EOS are comparable. The results are at low Pressure. At high pressures new EOS from give more accurate values as compared to SRK equation of state.

Conclusion

In comparison to the Soave-Redlich-Kwong (SRK) model and experimental data, this study validates a new equation of state (EOS) for carbon dioxide (CO₂). demonstrating its greater accuracy in forecasting PVT densities, particularly under high pressures. The results indicate that the EOS has the potential to improve efficiency and management in industrial settings, with wider implications for advanced thermodynamic modeling. This EOS may be extended to other gases in the future, which would increase its usefulness.

References

1. Mohagheghian, E., Bahadori, A., & James, L. A. (2015). Carbon dioxide compressibility factor determination using a robust intelligent method. Journal of Supercritical Fluids, 101, 140–149. https://doi.org/10.1016/j.supflu.2015.03.014

- 2. Sterner, S. M., & Pitzer, K. S. (1994). An equation of state for carbon dioxide valid from zero to extreme pressures. In Contrib Mineral Petrol (Vol. 117). Springer-Verlag.
- 3. Holland, T., & Powell, R. (1991). A Compensated-Redlich-Kwong (CORK) equation for volumes and fugacities of CO2 and H2O in the range 1 bar to 50 kbar and 100?1600C. Contributions to Mineralogy and Petrology, 109(2), 265–273. https://doi.org/10.1007/BF00306484
- 4. Bazile, J.-P., Nasri, D., Saley Hamani, A. W., Galliero, G., & Daridon, J.-L. (2018). Excess volume, isothermal compressibility, isentropic compressibility, and speed of sound of carbon dioxide + n-heptane binary mixture under pressure up to 70 MPa. I Experimental Measurements. The Journal of Supercritical Fluids, 140, 218–232. https://doi.org/10.1016/j.supflu.2018.05.028
- 5. Giordano, V. M., Datchi, F., & Dewaele, A. (2006). Melting curve and fluid equation of state of carbon dioxide at high pressure and high temperature. The Journal of Chemical Physics, 125(5).
- 6. https://doi.org/10.1063/1.2215609
- 7. Harvey, A. H., & Lemmon, E. W. (n.d.). New Reference Equation of State for Carbon Dioxide.

Authors -

Nida Tasneem is an MS student at the Chemical Engineering Department of King Fahd University of Petroleum & Minerals, Dhahran. She has a BS in Chemical Engineering from UET, Lahore, Pakistan. She has current research focuses on catalysis, particularly optimizing FCC catalysts using hierarchical zeolites, and molecular simulations to enhance propylene yield.

Dr. Shakeel Ahmed is a Research Scientist at the IRC for Refining & Advanced Chemicals, King Fahd University of Petroleum & Minerals. He specializes in industrial catalysis, inorganic synthesis, and instrumental analysis. With 200+ publications and 77 patents, his research advances catalytic processes. He is recognized among the top 2% of scientists worldwide.

Synthesis of Aluminum Modified Sulfonated Activated Carbon for Phenol Removal from Water

Faisal M. Alissa^{1,*}, Abdullah A. Alzahrani², Abdualilah I. Albaiz¹, Saroj K. Panda³

Aramco, EXPEC ARC, Dhahran, Saudi Arabia

² Aramco, Northern Area Technical Support Department, Tanajib, Saudi Arabia

Abstract

The treatment of oilfield-produced water remains a significant challenge due to the presence of soluble organic contaminants such as phenol. This study explores the synthesis and application of aluminummodified sulfonated activated carbon (Al-SAC) for phenol removal from water. Activated carbon was chemically modified through sulfonation, followed by the incorporation of aluminum to enhance adsorption efficiency. The synthesized adsorbent was characterized using X-ray diffraction (XRD), Brunauer-Emmett-Teller (BET) surface area analysis, and scanning electron microscopy (SEM-EDS). adsorption performance of Al-SAC was evaluated through batch adsorption experiments, and the results were analyzed using adsorption isotherm models. The studv demonstrated that aluminum modification significantly improves phenol adsorption capacity compared to unmodified activated carbon. These findings contribute to developing efficient and sustainable water treatment solutions for industrial applications.

Introduction

Although water is covering 70% of the world, not all of it is suitable for human consumption.

Many water sources require treatment prior to utilization. One type of water is the oilfield produced water. This water is considered a byproduct of the production process and is associated with several challenges such as organic corrosion, and scale formation. Dispersed oil in water can be removed by conventional means such as chemical demulsification, centrifuging...etc. However, soluble removal is more challenging. As elucidated by Zheng et al., (2016), offshore operations discharging-limit focuses on dispersed hydrocarbon parameters rather soluble content. However, as per the OSPAR Commission (2012), more focus should be given to the water-soluble organic chemicals. As of today, produced water re-injection to support the reservoir pressure stands out as the most feasible and environmentally friendly application as it reduces the need for alternative water sources. Although produced water associated with many challenges, the oil and gas industry are now perceiving it differently. Several studies were conducted on the use of produced water for metal extraction, and in irrigation after certain treatments. Therefore, produced water is turning from the re-injection stream to a valuable resource.

³ Aramco, Research & Analytical Services Department, Dhahran, Saudi Arabia ^{*} Corresponding author; email: faisal.alissa@aramco.com

biological, and physicochemical Many processes were implemented to treat produced water. Biological treatment processes demonstrated greater efficiency in removing a wide-range of water-soluble organic matter, with lower operational expenditures compared to the latter. Yet, high salinity produced water may be prone to such treatments as it can inhibit various biological activities. Adsorption is a process in which contaminants are trapped on the surface of a solid material. This is considered one of promising approaches to treating produced water. Oilfield produced water contains high levels of phenolic compounds that can reach up to 950 mg/L. Several adsorbents have been previously experimented for phenolic compounds removal such as: lignite (10 mg/g), activated carbon with surface area around 1,000 m2/g (300 mg/g), bentonite (1.7 mg/g), natural clay 11.1 mg/g, activated natural clay 18.9 mg/g, bamboo charcoal (24.96 mg/g), coconut shell charcoal (21.22 mg/g), coal charcoal (20.14 mg/g).

Activated carbon is widely recognized for its high surface area and adsorption properties, making it a popular choice for water treatment applications. However, enhancing its adsorption capacity and selectivity for specific contaminants remain a key research focus. Chemical modification carbon of activated can introduce functional groups that enhance performance. This article explores the synthesis and application of aluminum sulfonate modified activated carbon for the removal of phenolic compounds from water.

Sulfonation of activated carbon introduce sulfonic acid groups (RSO₂OH), enhancing the material's hydrophilicity. Additionally, this modification allows the material to hold various metals that can potentially improve the adsorption of polar organic compounds such as phenol. Metal attachment can manifest positive charges onto the surface of the material; thus, enhancing the affinity toward several organic pollutants (e.g., phenol). The primary objective of this research is to synthesize metals-modified sulfonated activated carbon, evaluate the adsorption performance for phenol removal, and compare the obtained efficiency with non-modified activated carbon. This study contributes to more effective solutions for water treatment in the oil and gas industry through understanding the underlying adsorption mechanisms.

Materials and Methods

Materials. The chemicals and reagents employed in this work were used without further purification. Sulfuric Acid 98% and 90% phenol solution in water were acquired from Fischer-scientific. Activated carbon was purchased from Kansai Coke & Petrochemicals Ltd. Anhydrous Aluminum Chloride (98%), Methanol (99.9%, anhydrous) and Dichloromethane (99.8%) were purchased from Sigma-Aldrich.

Synthesis of Aluminum Modified Sulfonated Activated Carbon (Al-SAC). Activated carbon was modified with sulfuric acid (H₂SO₄) to attach sulfonic acid groups onto the surface of the carbonaceous material.

The modification is done by mixing and heating the concentrated sulfuric acid under nitrogen gas flow at 120 °C as shown in Figure 1. The resulting slurry is then washed with deionized water thoroughly, methanol, then dichloromethane, finally left to dry in the oven at 90 °C. Sulfonic acid modified activated carbon (SAC) was then added onto a solution of 5% aluminum (III) chloride in methanol. Finally, the material was dried in the oven for 3 hours at 90 °C.

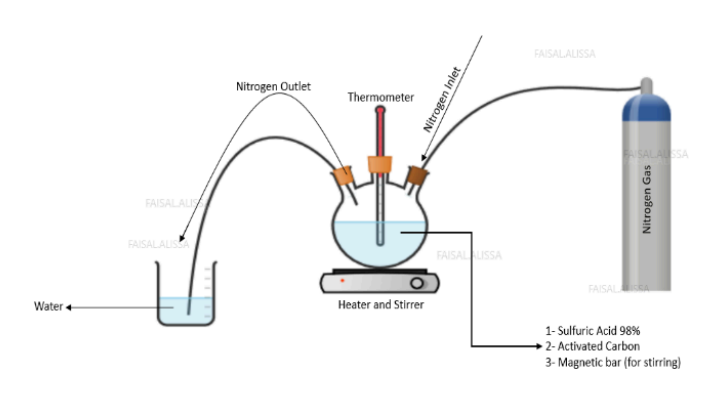


Figure 1. Apparatus for synthesis of sulfonic acid modified activated carbon.

Characterization. The Starting material, and all modified materials were crushed and placed on PANalytical X'Pert Pro MRD sample holder. Shimadzu XRD-7000 X-Ray Diffractometer was used with a cobalt x-ray tube. The diffraction data were collected from 0 to 85 degrees 2θ Bragg angles with a step size of 0.04 degrees and counting time of 1 degree per minute. Afterwards, the materials were analyzed using ASAP 2010 analyzer for Brunauer-Emmett-Teller (BET) surface area measurements. Then, the morphology of the materials was analyzed through scanning electron microscope energy dispersive spectroscopy (SEM-EDS) using ThermoFisher Helios 5 CX DualBeam system.

Phenol Analysis. Liquid chromatographic separations were carried out on an Agilent 1260 HPLC system with a binary pump, a degasser, an auto sampler, and a Diode Array Detector (DAD) set to record UV spectra from 200 nm to 400 nm. Instrument control, data recording, and data analysis performed using the OpenLab software, Agilent Technologies. Eclipse XDB-C18 column (150 x 4.6 mm) from Agilent Technologies was used for the separation. The average particle size for the used silica was 5 µm. A mixture of methanol and 0.1% formic acid in water (50:50, v/v) was used as the mobile phase. The detector was set at 275 nm to monitor elution of phenol from the column.

Batch Adsorption **Experiments.** ΑII experiments were conducted in a 100 mL beaker containing 50 mL aqueous solution of phenol at variable concentrations. A preweighed amount of an adsorbent is added to the beaker while stirring the solution. All experiments were carried out at room temperature. A sample of the solution was collected after 10, 20, 30, 40, and 50 minutes. Each sample was then analyzed Performance using High Liquid Chromatography (HPLC) to monitor the concentration of the analyte.

Adsorption Isotherms & Kinetics. Adsorption isotherm models describe the relationship between the adsorbate and adsorbent by identifying the adsorption mechanism. The following adsorption isotherms have been investigated in this work to identify the effect of various metals on the adsorption behavior.

(1) Langmuir adsorption isotherm is a twoparameter model suggesting a mono-layer adsorption on the surface of the material. The favorability of Langmuir adsorption is determined by the separation factor R_L. Equations 1 and 2 can be used to calculate the parameters of this model. (2) Freundlich adsorption isotherm is a model which describes the adsorption heterogeneous surface and defines the exponential distribution of active sites. Freundlich's formula is described in Equation 3, KF is Freundlich isotherm constant, 1/n is the adsorption intensity which also indicates the relative distribution of the energy and the heterogeneity of the adsorbent sites. The Freundlich maximum adsorption capacity can be calculated through Equation 4. Temkin adsorption isotherm is a unique model which considers the adsorbateadsorbent interactions on the adsorption process. This model assumes that the heat of adsorption (ΔH ADSORPTION) decreases the adsorbent's linearly as coverage increases. Equation 5 describes Temkin's model isotherm. KT is Temkin's isotherm constant, R is the universal gas law, b is a parameter related to the heat of sorption, and T is the temperature.

The kinetics of an adsorption process is a measurement of rate of adsorption per unit time. Varying the metal specie on the surface of the material can vary the kinetics of the adsorption process. Therefore, the adsorption kinetics of each material was investigated using the following models: (1) Pseudo-First Order (PFO) also known as Lagergren's rate equation is a kinetic model which represents a type of adsorption mechanism which is a bi-molecular reaction made to be unimolecular by increasing the concentration of one of the substrates.

To further elaborate, the adsorption is dependent on the concentration adsorbate because the binding sites on the adsorbent are assumed to be many and therefore expressed as excess of the second substrate. PFO is shown in Equation 6. Q_e is the experimental adsorption capacity at equilibrium, whereas Q_t is the adsorption capacity at time t. K is the rate of adsorption. In this model, Qe should be similar to Q_{THEORITICAL} given from the best fitted isotherm model. (2) Pseudo-Second Order (PSO) is a kinetic model which the adsorption rate is described proportional parameter to the binding sites on the surface of the adsorbent; therefore, is dependent on the concentration of the adsorbate in the surface of the adsorbent, and the adsorption driving force described as Q_{EOUILIBRIUM} - Q_{TIME} is an indicative of the surface coverage of the adsorbent. PSO is shown in Equation 7.

Results and Discussion

Brunauer-Emmett-Teller (BET). BET is an experiment in which the surface area of a material is estimated by the amount of adsorbed Nitrogen at different pressures at a temperature of 77K. The Activated Carbon (AC) used in this work as the backbone material has a high surface area (2947) m²/g). After every step of modification, a BET experiment was performed to measure the surface area. The results of these experiments are shown in Figure 2 (a) and the volume of adsorbed Nitrogen as a function of relative pressure is plotted in Figure 2 (b). After every surface modification a decrease in the BET surface area was noticed which is expected when adding a chemical-group to a surface. Functionalization of AC with sulfonic acid groups showed a slight drop in area to $2,600 \text{ m}^2/\text{g}$.

However, further functionalization with aluminum have resulted in higher drop in surface area. Al-SAC showed a surface area of 1817 m²/g. The significant decrease in the surface area by upon addition of aluminum may be attributed to the large-size of the metal which covered a portion of the adsorbent's surface. Thus, indicating that the surface was successfully modified.

Table 1. Equations of various adsorption isotherm models

Equation 1: Langmuir separation factor.

$$R_L = \frac{1}{1 + K_L C_o}$$

Equation 2: Langmuir adsorption isotherm.

$$\frac{C_e}{q_e} = \frac{1}{q_m K_e} + \frac{C_e}{q_m}$$

Equation 3: Freundlich adsorption isotherm.

$$\log q_e = \log K_F + \frac{1}{n} \log C_e$$

Equation 4: Freundlich's adsorption coefficient.

$$K_F = \frac{q_m}{C_o^{1/n}}$$

Equation 5: Temkin adsorption isotherm.

$$q_e = \frac{RT}{b} \ln K_T + \frac{RT}{b} \ln C_e$$

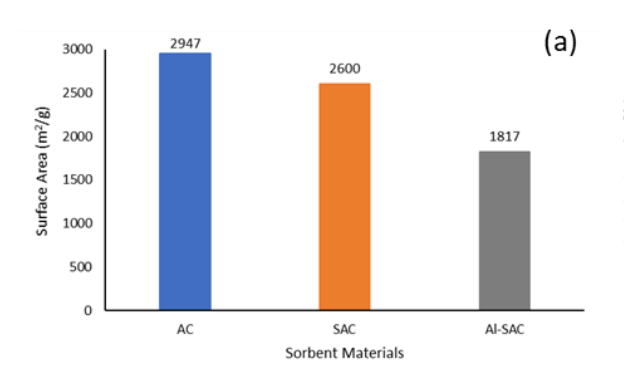
Table 2. Equations of various adsorption kinetics models

Equation 6: Pseudo-first order adsorption kinetics model.

$$\ln(q_e - q_t) = \ln q_e - k_1 t$$

Equation 7: Pseudo-second order adsorption kinetics model.

$$\frac{t}{Q_t} = \frac{1}{KQ_e^2} + \frac{t}{Q_e}$$



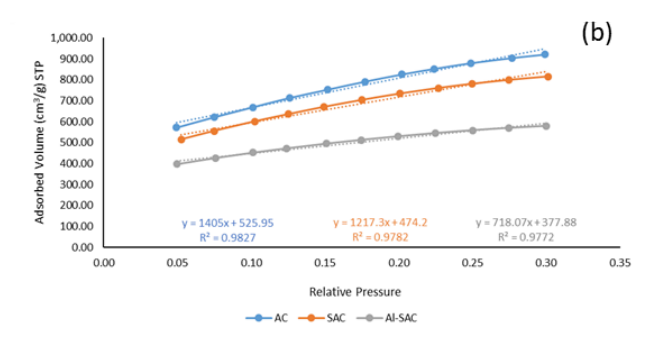


Figure 2. (a) BET surface analysis of the synthesized materials. (b) Nitrogen adsorption by the materials

X-Ray Diffraction (XRD). XRD is widely used technique in phase identification of a crystalline material. Activated carbon is an amorphous material that shows humps rather than peaks. However, the surface modification can be noticed in the spectra provided in Figure 3. The Activated Carbon (AC) initially shows a hump near 47 degrees which can be seen in the other two spectra. In the Sulfonic Acid - Activated Carbon (SAC) spectrum, a hump at 25 degrees was intensified vertically horizontally, which may be due to an overlap with the newly added Sulfonic Acid groups on the surface of the AC. The Aluminum modification was clearly shown due to an intensification at a low angle, nearly 15 degrees on the spectrum of Al-SAC.

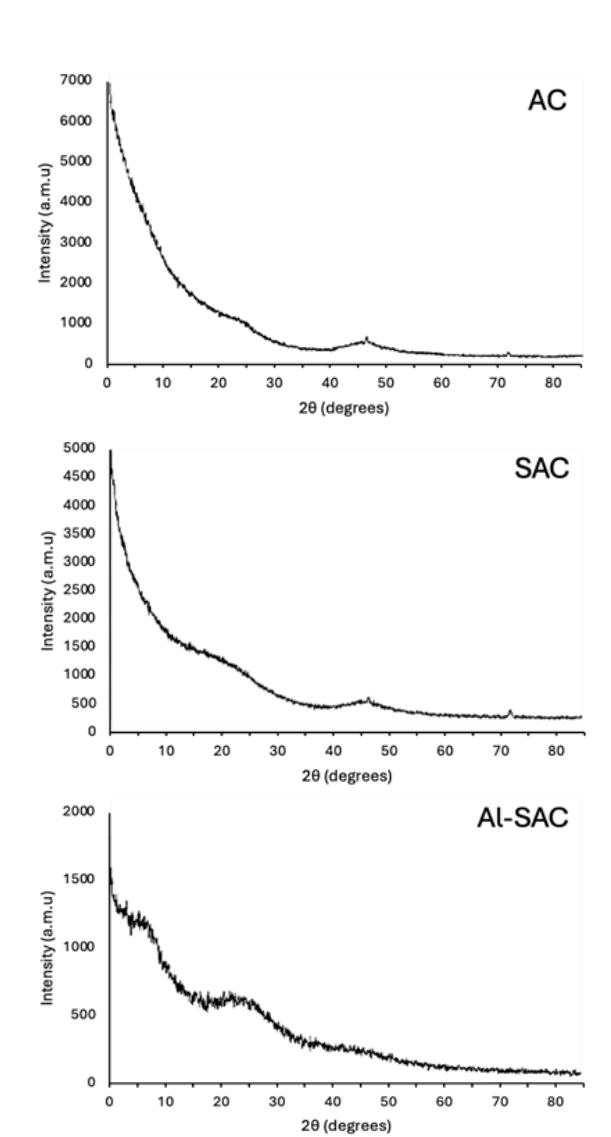


Figure 3. X-Ray Diffraction (XRD) for AC, SAC, and Al-SAC

Composition (EDX). The Elemental elemental composition was studied using Energy Dispersive X-Ray (EDX) through averaging scans of multiple sites. The results are provided in Table 1. A significant increase in the oxygen content as well as detection of sulfur in the first modification (SAC) may be attributed to a successful sulfonation of the AC. Although the surface of AC contained traces of oxygen, it increased by 6.72% while sulfur was detected at a percentage of 2.69%. The ratio of added-oxygen to sulfur is 2.5, while the actual ratio of oxygen to sulfur in sulfonic acid group (SO₃H) is 3.0 which may

indicate that there are other sulfurcontaining functional groups on the surface of the AC (e.g., sulfide (SH), or sulfinic acid (SO_2H)). Further functionalization using aluminum chloride showed aluminum content of 2.37% compared to 2.25% of sulfur. An approximate ratio of 1:1 is noticed which may be attributed to the aluminum sulfonate groups at the surface of AC.

Table 3. Equations of various adsorption isotherm models

Sorbent/ Element	Carbon (%)	Oxygen (%)	Sulfur (%)	Aluminum (%)	Silicon (%)	Chloride (%)
AC	97.78	1.51	N/A	N/A	0.71	N/A
SAC	88.11	8.23	2.69	N/A	0.97	N/A
Al-SAC	86.89	6.46	0.25	2.37	1.45	0.58

Morphological Analysis (SEM). Scanning Microscope Electron is an advanced instrument in which the surface of a material is scanned by a beam of electrons and the reflection of electron signals of different intensities produces an image of the material surface. This instrument is used to analyze the morphology on the surface a material and can be used to study the elemental composition of a material through the energy dispersive spectroscopy (EDS). Figure 4 shows the surface of each of the four materials, Activated Carbon (AC), Sulfonated activated carbon (SAC), and Aluminum modified sulfonated activated carbon (Al-SAC). The surface of the activated carbon illustrated randomly distributed particulates with rough texture and large voids. The chemical modifications have resulted in decreasing the surface area as shown in the BET results presented in Figure 2 (a). Yet, the surface morphology of the functionalized sorbents was not significantly altered. The pores and voids present at the surface of the activated

carbon were not compromised by the chemical modifications.

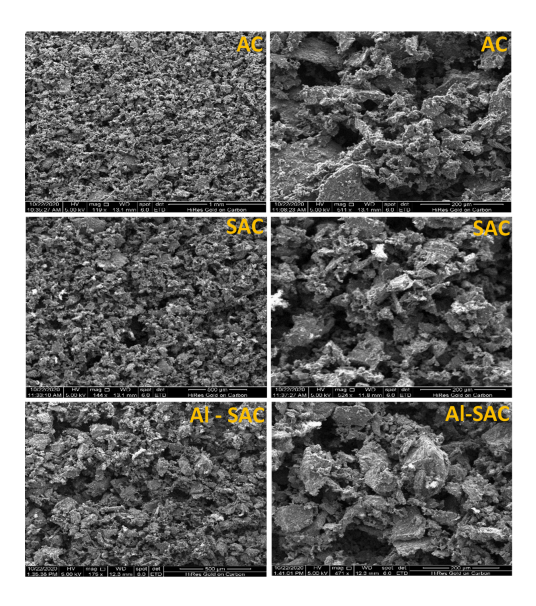


Figure 4. Scanning Electron Microscope (SEM) of AC, SAC, and Al-SAC.

Evaluation of Adsorption Performance

Activated Carbon (AC). The adsorption isotherm of the activated carbon showed an excellent correlation with Langmuir adsorption model as shown in Figure 5 (a). Both Equations 1 and 2 were used to calculate Langmuir maximum adsorption capacity Qm, and the separation factor R_I. Langmuir's maximum adsorption capacity of phenol onto the activated carbon was found throughout the experimentation and calculations as 2,500 milligrams per gram of sorbent. This high uptake is considered phenomenal for pollutants removal from water. Nevertheless, the separation factor of the adsorption system is 0.54; thus, the adsorption is considered favorable according to the model. All Langmuir parameters are provided in Table 4.

The kinetics of the adsorption system was best fitted in Lagergren's, Pseudo-First Order model which is shown in Equation 6. In Figure 5 (b) a plot of Lagergren's model for phenol onto activated carbon is shown at different concentrations of phenol. Similarly, all Lagergren's parameters are provided in Table 4. The theoretical adsorption capacity of Lagergren's model was found to be increasing with respect to the concentration of phenol; however, the average was found to be 2845 mg/g which close to the adsorption capacity calculated using Langmuir's adsorption model. isotherm Nonetheless. the calculated adsorption capacity for the adsorption of 1,000 ppm of phenol was 1,892 mg/g which is greater than the experimented concentration. Similarly, Qe at a phenol concentration of 2,000 ppm was 2,524 mg/g. These values may indicate that the surface has not been fully covered yet. The gap between the two values continue to shrink further when experimented at a phenol concentration of 3,000 ppm, the calculated maximum adsorption capacity at equilibrium was 3,030 mg/g. This value appears as a turning point of the adsorption capability of the material where the surface coverage has been almost reached due to the low gap between the two values. Qe started to become less than the starting phenol dose at concentrations higher than 4,000 ppm, yet continued to increase. Which indicates that the phenol coverage on the surface stretchable and directly proportional to the concentration of the analyte.

Table 4. Adsorption parameters of phenol onto activated carbon.

	adsorption herm	Pseud	o-First Orde	r adsorption k	inetics
Q _m (mg/g)	2500	[Phenol]	K_{PFO} ($\frac{mg}{gxmin}$)	Q_E (mg/g)	R ²
K _L (_{I/mg})	0.00042	1000	0.0308	1892	0.9994
R_L	0.54	2000	0.1077	2524	0.9999
R ²	0.9828	3000	0.0756	3030	0.9915
		4000	0.0541	3129	0.9930
		6000	0.026	3650	0.9957

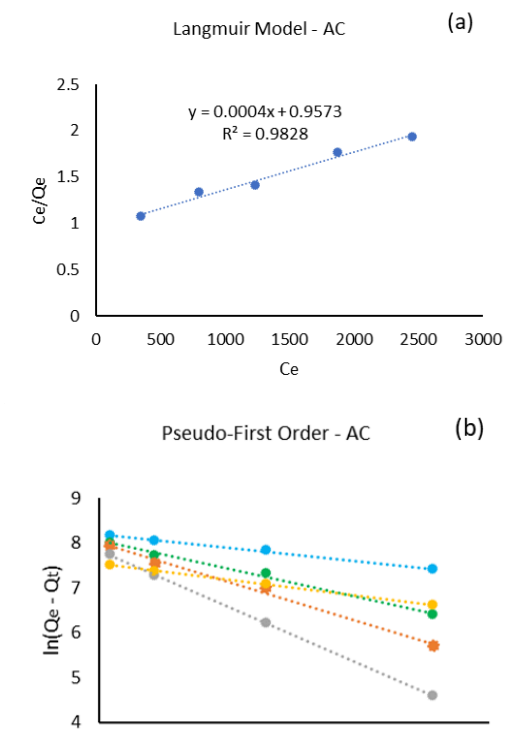


Figure 5. Phenol adsorption onto AC fitted with (a) Langmuir isotherm, and (b) Pseudo-First Order models

20

Time

• 4000 ppm

• 1000 ppm

30

3000 ppm

0

5000 ppm

2000 ppm

Sulfonated Activated Carbon (SAC). The sulfonated activated carbon adsorption isotherm showed a high correlation with Temkin adsorption model as shown in Figure 6 (a). Equation 5 was used to calculate Temkin's isotherm constant K_T and b which is related to the heat of adsorption. All Temkin's isotherm parameters are provided in Table 5.

The variation in the adsorption isotherm between the SAC and AC is a result of the chemical modifications. Temkin's isotherm model is not describe the adsorption behavior (physical/chemical) nor provide insight on the maximum adsorption capacity. Thus, the two sorbents can be compared only through the adsorption capacity at equilibrium. The kinetics of phenol adsorption by SAC was best fitted using Pseudo-Second Order (PSO) model which is shown in Equation 7. In Figure 6 (b) a plot of Pseudo-Second Order model is shown at different concentrations and the kinetic parameters are calculated and provided in Table 5. The theoretical adsorption capacity of Pseudo-Second Order model was found to be increasing with respect to the concentration of phenol; however, the average was found to be 850 mg/g which is extremely less than AC. Sulfonic acid functionalization promoted the presence of negative charges at the surface of the carbonaceous sheet. Thus, may have reduced the favorability of surface interactions between the two materials.

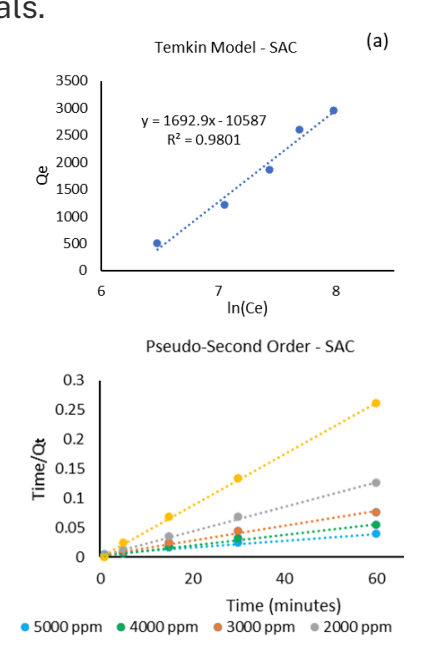


Figure 6. Phenol adsorption onto SAC fitted with (a) Temkin isotherm, and (b) Pseudo-Second Order models

Table 5. Adsorption parameters of phenol onto sulfonic acid modified activated carbon

	Temkin adsorption isotherm		o-Second Ord	er adsorption	kinetics
K _T (_{L/g})	0.0019	[Phenol]	K_{PSO} ($\frac{mg}{gxmin}$)	Q _E (mg/g)	R ²
B (J/mg)	1.4635	1000	9.68 x 10 ⁻²	227	0.9992
R ²	0.9801	2000	1.76 x 10 ⁻³	476	0.9979
		3000	4.80 x 10 ⁻⁴	833	0.9944
		4000	7.11 x 10 ⁻⁴	1250	0.9995
		5000	6.43 x 10 ⁻⁵	1666	0.9899

Aluminum Modified SAC (Al-SAC). The aluminum modified sulfonated activated carbon (Al-SAC) adsorption isotherm showed exceptional correlation Freundlich's adsorption model as shown in Figure 7 (a). Both Equation 3 and Equation 4 were used to calculate Freundlich's maximum adsorption capacity Qm which found to be 2593 mg/g and Freundlich's adsorption intensity 1/n and adsorption constant KF, all Freundlish's parameters are provided in Table 6. The kinetics of Phenol adsorption onto Al-SAC was best fitted with Pseudo-Second Order model which is shown in Equation 7. In Figure 7 (b) a plot of Lagergren's model is shown at different concentrations and Lagergren's parameters are provided in Table 6. The theoretical adsorption capacity of Lagergren's model was found to be increasing with respect concentration of Phenol, however average was found to be 2475.8 mg/g which is similar to the adsorption capacity in Langmuir's model.

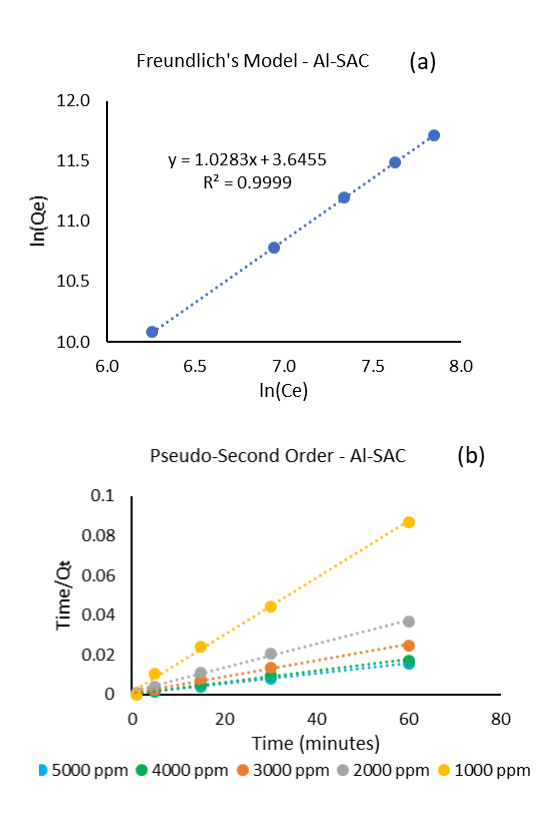


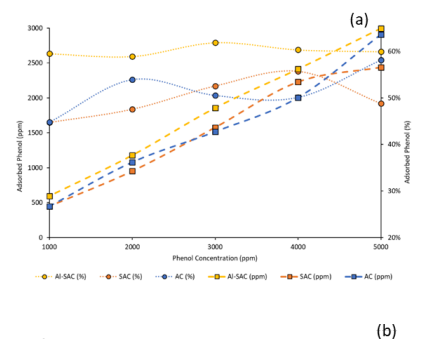
Figure 7. Phenol adsorption onto Al-SAC fitted with (a) Freundlich isotherm, and (b) Pseudo-Second Order models

Table 6. Adsorption parameters of phenol onto aluminum modified sulfonic acid activated carbon.

Temkin adsorption isotherm		Pseud	o-Second Ord	er adsorption	kinetics
K _F (L/mol)	38.30	[Phenol]	$K_{PSO}\left(\frac{mg}{gxmin}\right)$	Q_E (mg/g)	R ²
Q _M (_{mg/g})	2593	1000	1.40 x 10 ⁻³	714	0.9998
R ²	0.9999	2000	2.57 x 10 ⁻⁴	1666	0.9962
n	0.97	3000	2.29 x 10 ⁻⁴	2500	0.9974
		4000	1.80 x 10 ⁻⁴	3333	0.9950
		5000	1.33 x 10 ⁻⁴	4166	0.9971

Adsorption Selectivity Enhancement. Phenol adsorption via AC was in alignment with Langmuir's adsorption isotherm model. Yet, followed Temkin's isotherm model when the AC was sulfonated. Both models

indicate a physical adsorption mechanism. This may be the reason behind the poor adsorption selectivity at lower concentrations by both materials, as shown in Figure 8 (a). At a phenol concentration of 1,000 ppm, the adsorption percentage by both AC, and SAC was 45%. Whereas the adsorption percentage by Al-SAC at the same concentration was 60%. At higher phenol concentrations, all materials showed greater adsorption performance including AC, reaching to 58% of 5,000 ppm of phenol (2,900 ppm adsorbed). Yet, Al-SAC's adsorption performance remained steady at 60% (3,000 ppm). Although the adsorption is considered lower, it remained almost steady throughout the studied analyte concentration range. These data illustrate that the backbone material (AC) has a maximum adsorption percentage of around 60% in a solution; however, this percentage is susceptible to decay at lower analyte concentrations. Functionalization of the surface with aluminum-sulfonate groups has maintained the selectivity in solution at variable analyte concentrations. Although the functionalization steps reduced the surface area of the material, Al-SAC has slightly increased its performance when compared to its backbone (AC). The adsorbed mass of phenol per area of sorbent can provide insight on the adsorption selectivity [16]. Therefore, the data from this study were used to construct Figure 8 (b) which shows the adsorption per surface area of sorbent at various analyte concentrations. The performance of the two initial materials (AC, SAC) are almost overlapping. However, the Al-SAC stands out of the group with greater performance. This indicates that the selectivity of phenol adsorption was enhanced on the surface of the sulfonated activated carbon when adding Aluminum species.



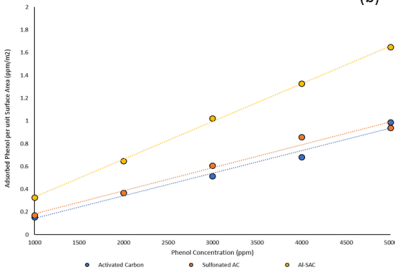


Figure 7. Assessment of adsorption selectivity through (a) amount of adsorbed phenol by 1 milligram of sorbent in different sorbate concentrations, and (b) phenol adsorption per unit area at different concentrations

Conclusion

The performance of several carbonaceous materials in the adsorption of water-soluble organic contaminants such as phenol has been investigated and showed maximum adsorption capacities. Sulfonic acid modified activated carbon (SAC) can hold various metals such as aluminum. The presence of the metal has significantly changed the performance of the adsorption from kinetic and isotherm perspectives. Nonetheless, it has enhanced the selectivity of adsorption even when the surface area is compromised. In this work, aluminum sulfonate modified activated carbon (Al-SAC) was derivatized from activated carbon (AC). The derivatization has reduced the surface area by 38.3%. Yet, the maximum adsorption capacity of Al-SAC was 2593 mg/g which is slightly greater than the backbone 2,524 mg/g, and the adsorption percentage became almost steady at 60% in both low and high analyte concentrations. Which was a challenge for the pristine material as the adsorption percent was

varying between 45 – 58%. This indicates that this chemical modification has resulted in an enhancement of the adsorption selectivity of phenol onto the surface of the sorbent.

References

- 1. Mishra, Rakesh Kumar. "Fresh water availability and its global challenge." British Journal of Multidisciplinary and Advanced Studies 4, no. 3 (2023): 1-78.
- 2. Theurer, Jared, Oluwatobi Ajagbe, Jhouly Osorio, Rida Elgaddafi, Ramadan Ahmed, Keisha Walters, and Brandon Abbott. "Removal of residual oil from produced water using magnetic nanoparticles." SPE Journal 25, no. 05 (2020): 2482-2495.
- 3. Zheng, Jisi, Bing Chen, Worakanok Thanyamanta, Kelly Hawboldt, Baiyu Zhang, and Bo Liu. "Offshore produced water management: A review of current practice and challenges in harsh/Arctic environments." Marine pollution bulletin 104, no. 1-2 (2016): 7-19.
- 4. OSPAR Commission. 2012. OSPAR Recommendation 2012/5, Risk Based Approach to the Management of Reduced Water Discharges from Offshore Installations: Decisions, Recommendations & Agreements, https://www.ospar.org/convention/agreements (accessed 29 May 2018).
- 5. Lusinier, Nicolas, Isabelle Seyssiecq, Cecilia Sambusiti, Matthieu Jacob, Nicolas Lesage, and Nicolas Roche. "Biological treatments of oilfield produced water: A comprehensive review." SPE Journal 24, no. 05 (2019): 2135-2147.

- 6. Jang, Eunyoung, Yunjai Jang, and Eunhyea Chung. "Lithium recovery from shale gas produced water using solvent extraction." Applied Geochemistry 78 (2017): 343-350.
- 7. DuChanois, Ryan M., Nathanial J. Cooper, Boreum Lee, Sohum K. Patel, Lauren Mazurowski, Thomas E. Graedel, and Menachem Elimelech. "Prospects of metal recovery from wastewater and brine." Nature Water 1, no. 1 (2023): 37-46.
- 8. Kumar, Amit, Hiroki Fukuda, T. Alan Hatton, and John H. Lienhard. "Lithium recovery from oil and gas produced water: a need for a growing energy industry." ACS Energy Letters 4, no. 6 (2019): 1471-1474.
- 9. Dolan, Flannery C., Tzahi Y. Cath, and Terri S. Hogue. "Assessing the feasibility of using produced water for irrigation in Colorado." Science of The Total Environment 640 (2018): 619-628.
- 10. Echchelh, Alban, Tim Hess, and Ruben Sakrabani. "Reusing oil and gas produced water for irrigation of food crops in drylands." Agricultural Water Management 206 (2018): 124-134.
- 11. Andrade, V. T., B. G. Andrade, B. R. S. Costa, O. A. Pereira Jr, and M. Dezotti. "Toxicity assessment of oil field produced water treated by evaporative processes to produce water to irrigation." Water Science and Technology 62, no. 3 (2010): 693-700.
- 12. Polat, Hürriyet, Murat Molva, and Mehmet Polat. "Capacity and mechanism of phenol adsorption on lignite." International Journal of Mineral Processing 79, no. 4 (2006): 264-273.

13. Banat, F. A., Bilal Al-Bashir, S. Al-Asheh, and O. Hayajneh. "Adsorption of phenol by bentonite." Environmental pollution 107, no. 3 (2000): 391-398.

14. Djebbar, M., F. Djafri, M. Bouchekara, and A. Djafri. "Adsorption of phenol on natural clay." Applied Water Science 2 (2012): 77-86.

15. Ma, Yan, Naiyun Gao, Wenhai Chu, and Cong Li. "Removal of phenol by powdered activated carbon adsorption." Frontiers of Environmental Science & Engineering 7 (2013): 158-165.

16. [1] Xie, Bingxin, Jihong Qin, Shu Wang, Xin Li, Hui Sun, and Wenqing Chen. "Adsorption of phenol on commercial activated carbons: modelling and interpretation." International Journal of Environmental Research and Public Health 17, no. 3 (2020): 789.

17. Ramírez, Eduardo Enrique Pérez, M. de la L. Asunción, Veronica Saucedo Rivalcoba, Ana Laura Martínez Hernández, and Carlos Velasco Santos. "Removal of phenolic compounds from water by adsorption and photocatalysis." Phenolic Compounds — Natural Sources, Importance and Applications (2017).

18. Alissa, Faisal M., Dauda Mohammed, Abdalghaffar M. Osman, Chanbasha Basheer, Mohammad Nahid Siddiqui, Abdurrahman A. Al-Arfaj, and Munzir H. Suliman. "Synthesis of highly efficient asphalt-based carbon for adsorption of polycyclic aromatic hydrocarbons and diesel from emulsified aqueous phase." Carbon Letters 30 (2020): 555-567.

19. Ruthven, Douglas M. Principles of adsorption and adsorption processes. John Wiley & Sons, 1984

Authors -

Faisal M. Alissa is a researcher in oilfield chemistry at KAUST Upstream Research Center. His work focuses on flow assurance, water management, and wellbore stimulation. Faisal's scientific and operational contributions have resulted in 6 granted patents, and 7 papers within 5 years in the industry.

Dr. Saroj K. Panda is a Research Science Specialist at Aramco, leading the liquid chromatography lab. With 15+ years of experience, he specializes in characterizing petroleum hydrocarbons, refinery additives, and polymers using chromatography and mass spectrometry. He earned his Ph.D. from the University of Muenster, Germany, and has 30+ publications, 50+ conference presentations, and mentored 10+ young scientists.

Abdullah Alzahrani is a Lab Scientist at Aramco, in the Northern Area Producing Technical Support Department. He holds a Bachelor's degree in Chemistry from King Fahd University of Petroleum & Minerals (KFUPM). Abdullah has made notable contributions the field to of chromatography, with research papers published on size exclusion chromatography of aromatic compounds.

Abdualilah Albaiz is a researcher at EXPEC ARC, Aramco upstream research center, where he holds a B.Sc in Chemistry science. Abdualilah works focuses on the field of stimulation and oil field chemistry that includes scale prevention. He also worked in different departments within Aramco as Production Engineering and Reservoir Management.

Determination of Aliphatic Amines in Industrial Waste Water Using SPME

Talal M. Al-Ghamdi
Aramco, Technical Support Department, Abqiaq, Saudi Arabia
Author email: talal.ghamdi.3@aramco.com

Abstract

In the presence of dissolved oxygen in the water inside a pipeline, the oxygen attacks the steel to form iron oxides. To prevent this, corrosion inhibitors are added to the crude oil streams. These chemicals are amines-based that form a film to coat the steel and prevent it from contacting the oxygen. Amines residuals should be monitored in the system and this is classically done by liquid-liquid extraction (LLE) of amines followed by colorimetric determination using spectrophotometry.

In this work, solid phase microextraction (SPME), a novel extraction technique that uses no solvent, was used as a sample preparation technique to isolate the amines from the complex sample matrix and then the gas chromatography (GC) system was used for separation and quantification of amines. A flow-through system was used to simulate the process of flowing streams in pipelines during oil production.

A method was developed to determine amines residuals at the lowest detection limit possible at the optimized conditions such as solution pH, ionic strength, and sand contents. It was found that residuals can be determined as low as 1 ng/mL using the GC system equipped with a flame

ionization detector (FID). This method was developed in the lab using a model to simulate the flowing streams and containing synthesized waste water.

This method is an environmental friendly technique that will minimize the use of hazardous solvents and therefore the need for the proper disposal of them. Also it does not require pretreatment steps of samples or many reagents to be used in the extraction process of amines residuals. Finally, it will provide more precise results in a timely manner for better and quicker actions.

Introduction

The fundamental step of any analytical procedure is the sample preparation, which involves cleaning the sample matrix and transporting the target analytes to a more suitable matrix for instrumental analyses. This is very crucial because it leads to the achievement of better detection limits as compared of not having this step. Before obtaining any samples for analyses, sample preparation and a separation technique should be considered. The target analyte and the expected concentration govern the separation method for organic pollutants

was the solvent extraction prior to analysis, which was then replaced with solid phase extraction (SPE). Excessive use of organic solvents, which are costly and harmful to the environment, as well as extended time elapsed in the extraction process are two disadvantages associated with these traditional techniques.

Solid phase microextraction (SPME) is a sample preparation technique that was introduced in the 1990s by Professor Janusz Pawliszyn and developed in his research lab at the University of Waterloo. This technique, which can be used in the extraction of gases, liquids, and solids, has many advantages over other conventional extraction techniques like SPE and liquid-liquid extraction (LLE). SPME reduces the impact of harmful organic solvents to both humans and the environment.

The objective of this work is to develop and optimize an SPME method for the analysis of aliphatic long chain amines from a solution that has a similar matrix to that of industrial waste water. A flow-through system is used to generate a standard water solution at a constant flow rate in order to simulate flowing streams in pipelines.

Experimental Section

Decylamine $(C_{10}H_{21}NH_2),$ dodecylamine $(C_{12}H_{25}NH_2),$ and tetradecylamine $(C_{14}H_{29}NH_2)$ were purchased from Aldrich (Oakville, ON). HPLC grade methanol was used to make standards and was purchased from Caledon Laboratories Ltd. (Georgetown, ON). NANO-pure water that was used in the preparation of samples was obtained from Barnstead Ultrapure Water Systems (Dubuque, IA). Helium, nitrogen, and hydrogen were obtained from

Praxair (Waterloo, ON) and were of ultrahigh purity. High purity air was generated in the lab using a Whatman Zero Air Generator (Haverhill, MA). Sodium chloride (NaCl), sodium carbonate (Na₂CO₃), and sodium hydrogen carbonate (NaHCO₃) that was used to modify the solution matrix were purchased from Supelco (Oakville ON).

The 100 µm thickness PDMS coating fibers holder and assemblies used were purchased from Supelco (Oakville, ON) and were conditioned as recommended by the manufacturer. Graduated clear glass bottles (1 L) were used to prepare the solutions and were obtained from Cole-Palmer (Montreal, QC). Hamilton syringes that were used for standard preparation and injection were purchased from Hamilton (Reno, NV). Screw top amber glass vials (40 mL) with PTFE/silicone septa were used for the standards preparation and were obtained from Supelco (Oakville, ON).

A Varian CP-3400 GC equipped with a flame ionization detector (FID) obtained from J&W Scientific (Mississauga, ON) and an Optic 2 programmable-temperature vaporizing (PTV) injector obtained from ATAS GL (Veldhoven, Netherlands) was used for all experiments. The carrier gas was helium maintained at a pressure of 15 psi, and the detector gases flow rates were set to 300 mL/min for air, 25 mL/min for nitrogen (make-up gas), and 30 mL/min for hydrogen. A 1.0 internal diameter mm (ID) insert liner capable of handling injections of less than 3 µL was used for both SPME and liquid injection and was obtained from ATAS GL (Veldhoven, Netherlands).

The column used was a Restek Rtx®-5Sil MS (5% diphenyl/95% dimethylsiloxane) phase, and its dimensions were

15 m x 0.25 mm ID with 0.25 μm stationary phase thickness, which was purchased from Chromatographic Specialties (Brockville, ON). For the instrument method, the initial oven temperature was 50°C for 2.5 min, then ramped up to 280°C at the rate of 40°C/min. The injector temperature was programmed for solvent injection from 50°C to 270°C with a rate of 600°C/min and was kept at 270°C for the fiber desorption, and the detector temperature was held at 300°C.

A flow-through laboratory water system was used to simulate the flowing streams in pipelines and provide large sample volumes. A liquid chromatography (LC) pump capable of generating stable flow rates ranging from 0.01 to 9.99 mL/min was used to deliver solutions to a modified 40 mL vial that is connected to a waste container through Teflon tubes (Figure 1).

The flow rate of the LC pump was set at 5.0 mL/min. Solutions with a concentration of 0.1 μ g/mL, prepared by adding 0.2 mL of 500 μ g/mL methanolic amines mixture to 1 L of nano-pure water, were prepared in a 4 L bottle. The pump was then operated for several hours to allow the system to equilibrate before starting the extractions. Extracted masses were calculated from solvent injection calibration curves, and concentration of the amines mixture in the system was confirmed by LLE.

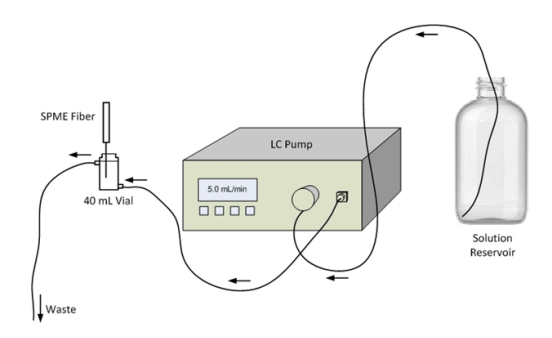


Figure 1. Schematic of the flow-through standard amines solution system

Results and Discussion

Although the flow-through system provides a good means of agitation, magnetic stirring was used as well to assist in the agitation process, by placing the 40 mL sampling vial on a stirrer with a speed of around 1,000 rpm. Then, to establish the extraction time profile, the fiber was exposed to the flowing stream in the 40 mL sampling vial for variable times, starting from 1 minute up to 300 minutes. Extraction at each time was repeated three times and relative standard deviation was calculated, which was in the range of 5%. Figure 2 is an example of the extraction time profile:

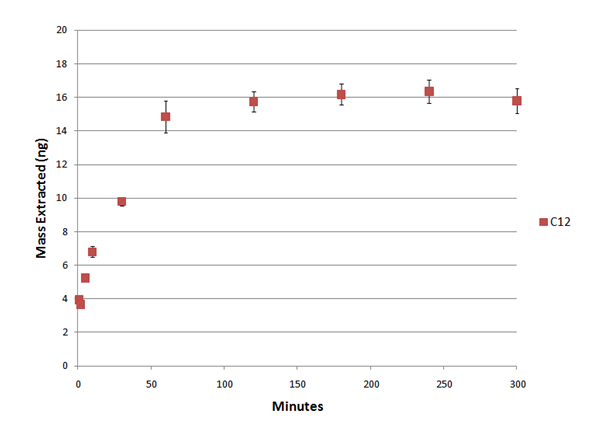


Figure 2. Extraction time profile of dodecylamine from flow-through system that contains amines mixture from 1 to 300 min.

Amines are bases that are easily protonated in neutral water and so become ionized. So, the pH of the solution should be adjusted to convert all species to their neutral form. This can be approached by alkalizing the solution to a pH two units above the pKa values of the analytes to assure that the dominant species in the solutions are neutral as per the Henderson-Hasselbalch relationship. 10,11,12,13 In the case of the analytes under study, the pKa values are around 10.60, so a pH adjustment should be 12.60.¹⁴ approximately made to Subsequently, extracting from solutions with extreme pH conditions, whether low or high, could damage the fiber coating.

Solutions were prepared by adding the amine standard mixture into water without pH adjustment and compared with a buffered solution that has the pH of 10. In both cases, solutions were prepared in bulk and the system was allowed to equilibrate before the start of extraction. Figure 3 shows a comparison between both cases.

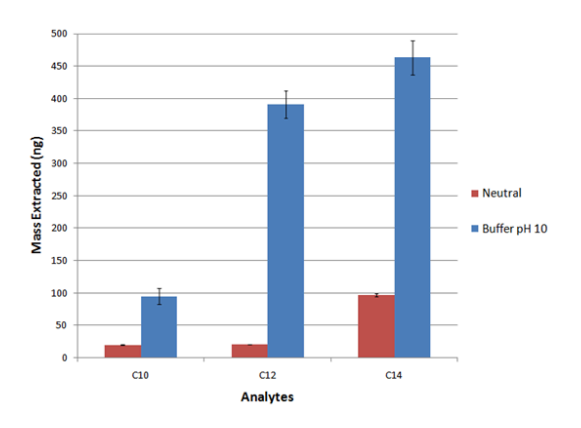


Figure 3. Comparison of extracted masses of different amines from neutral solution and pH-adjusted solution

It can be clearly seen that the amount extracted at a pH of 10 was substantially increased as compared to that of the neutral conditions. This is because more analytes were in the non-ionic form at a pH of 10 as compared to that of neutral conditions, so more analytes were available for extraction by the fiber coating. The pH adjustment was carried out for the rest of the experiments.

When salt is added to the solution, the ionic strength is increased resulting decreasing the solubility of the organic analytes and improving the sensitivity of the method. This is due to the fact that aqueous solutions prefer to solvate salts rather than organic matters which will result in enhancing the release of analytes from the sample and make them available for extraction by the fiber coating. The addition of NaCl was chosen to adjust the ionic strength of the solution, which is the most often used type of salt.

In all experiments, solutions were prepared by adding the same amounts of analytes to water, resulting in the same concentration, which was 0.1 µg/mL of the amines mixture. The system was allowed to run 12 hours to reach a steady state and to equilibrate before starting extractions. Extractions were carried out for 3 hours, which is the equilibration time for the heavier amine (tetradecylamine). Please refer to Figure 4 for the comparison.

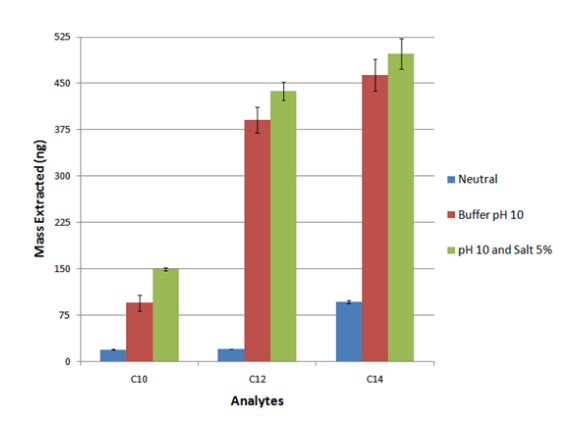


Figure 4. Comparison of extracted masses of different amines from neutral solution, pH 10 solution, and pH 10 solution with 5% NaCl.

The linearity of the PDMS coating to extract amines was determined by the analyses of a set of diluted solutions from the original concentration, which was 0.1 µg/mL using the optimized conditions. Several concentrations (5, 10, 25, and 50 ng/mL) were used for this experiment to establish the linear curve. Each concentration was prepared separately and allowed to run for a couple of hours in the system until it reached a steady-state before starting extractions. Each extraction was performed in triplicate, and RSD was calculated.

Table 1. Linearity of the Method with Calculated LOD

Compound	Fiber linear range (ng/mL, FID)	R²	RSD %	LOD (ng/mL)
Decylamine	5 – 100	0.9967	2.0 – 4.5	0.8
Dodecylamine	5 – 100	0.9992	3.3 - 5.3	1.3
Tetradecylamin	5 – 100	0.9976	1.2 - 5.0	1.0

The limit of detection (LOD) of the detector is generally defined as the lowest amount of analyte that could provide a signal three times the background noise of the blank. It can be calculated mathematically by running at least seven extractions of a blank or the lowest concentration that could be detected, and then a standard deviation of these runs is calculated and the limit of detection would be three times the standard deviation. For that purpose, a solution containing 1 ng/mL of amines mixture was prepared, and the experiment was carried out at optimized conditions. Calculated LODs are listed in Table 1.

Conclusion

In this paper, a method was developed for the extraction of decylamine, dodecylamine, and tetradecylamine from water, using a flow-through system. The various method development parameters were carefully studied and compared to get the optimum conditions for extraction. It was found that the pH of the sample has to be adjusted to 10 to have approximately equal ratios of dissociated and undissociated amines in the solution. This is because of the fact that the fiber coating extracts only analytes in the un-dissociated form. Sand addition was performed to analyze the possible losses of analytes due to the presence of another extraction phase.

It was found that some analytes might be lost if the sample contained certain amounts of sand, likely due to binding of analytes to it. The limits of detection of the three analytes were calculated from seven extractions of a sample contacting 1 ng/mL of amines.

References

- 1. Fontanals, N.; Marcé, R. M.; Borrull, F. J. Chromatogr. A. 2007, 1152 (1-2), 14-31.
- 2. Baltussen, E.; Cramers, C. A.; Sandra, P. J. F. Anal. Bioanal. Chem. 2002, 373 (1-2), 3-22.
- 3. Kloskowski, A.; Chrzanowski, W.; Pilarczyk, M.; Namiesnik, Crit. Rev. Anal. Chem. 2007, 37 (1), 15-38.
- 4. Aulakh, J. S.; Malik, A. K.; Kaur, V.; Schmitt-Kopplin, P. Crit. Rev. Anal. Chem. 2005, 35 (1), 71-85.
- 5. Dietz C.; Sanz, J.; Cámara, C. J. Chromatogr. A. 2006, 1103 (1), 183-192.
- 6. Pan, L.; Chong, M.; Pawliszyn, J. J. Chromatogr. A. 1997, 773 (1-2), 249-260.
- 7. Stashenko, E. E.; Martínez, J. R. Trends Anal. Chem. 2004, 23 (8), 553-561.
- 8. David R. Lide, Editor, Electronic Editions, CRC Handbook of Chemistry and Physics, 92nd ed., Internet Version 2012.

Author

Talal Al-Ghamdi is s professional scientist with 25 years of experience in the oil, gas and energy industry. Skilled in petroleum fingerprinting, water resource management, separation science, and oilfield chemicals characterization.

Published number of technical papers in international venues and granted a patent from USPTO. Talal holds MSc degree focused in Analytical Chemistry from University of Waterloo and currently working as laboratory manager at Aramco.



About Kalada

Kalada was founded in 2016 and is a fully Saudi-owned business. Our specialty is offering cutting-edge chemical solutions that are specifically designed to meet the demands of top businesses in sectors including energy, petrochemicals, gas, and oil.



Our Vision

To be a leading provider of catalysts, adsorbents, and water treatment solutions in the Middle East and Europe.



Our Mission

We are committed to delivering top-tier chemical solutions to our clients, focusing on quality, innovation, and sustainability.

Our Core Values



Commitment: Upholding the highest ethical standards.



Customer Service: Providing dedicated and professional support to our clients



Innovation: Driving excellence through creativity

Our Locations



Dammam

A warehouse spanning 2,200 square meters.



Khobar

Our headquarter.



Jubail

A 12,000-square-meter, cutting-edge industrial complex.

Why Choose Kalada



Over 8 years of experience in the field



innovative solutions aligned with Saudi Vision 2030.



A global supply network ensuring efficient service delivery to clients











Comprehensive Services

Specialized Chemicals:

- Refinery and Petrochemical Catalysts.
- Adsorbents: Activated Alumina, Molecular Sieves, Zinc Oxide, and Activated Carbon.
- Performance-enhancing additives for refined products.





Water Treatment and Oil Field Service

- Oil and gas well chemical solutions, including demulsifiers, corrosion inhibitors, and scale inhibitors.
- Comprehensive oilfield and water management services.



Recovering valuable metals from industrial waste streams.

Supervision of catalyst loading and operational start-up. Blending and repackaging of chemical materials.



Precious Metals Recovery Service:

Recovering valuable metals from industrial waste streams.

Stay connected by visiting our offices or contacting us via email or phone for further inquiries.







Green Catalytic Oxidation of Ethanol to Acetaldehyde Using Mentha spicata and Thymus vulgaris Extracts: A Sustainable Alternative to Metal Catalysts

Dr. Saad Althubyani
Educational Supervisor, General Directorate of Education in Makkah, Saudi Arabia
Author email: shalthobiani@hotmail.com

Abstract

study investigates the catalytic potential of plant-derived extracts (Mentha spicata [mint] and Thymus vulgaris [thyme]) for ethanol oxidation to acetaldehyde, a key transformation in organic synthesis. The catalytic activity of these extracts was evaluated under controlled conditions (50°C. 30 min reaction time) and compared to traditional metal catalysts (Ag/SiO₂, CuO). Gas chromatography-mass spectrometry (GC-MS) confirmed acetaldehyde formation, with mint extract achieving a conversion rate of 68.2% ± 2.5%, outperforming thyme (54.7% ± 3.1%) and approaching the efficiency of CuO catalysts (72.5% ± 1.8%). Kinetic studies revealed a lower activation energy for plant-based catalysts compared to nonbiological alternatives, suggesting promising green catalytic pathway. Scanning electron microscopy (SEM) and thermal analysis (TGA) assessed catalyst stability and morphology. The results demonstrate that plant-derived catalysts offer a sustainable and environmentally friendly alternative to conventional metal catalysts, with significant potential for industrial applications.

Introduction

The oxidation of ethanol to acetaldehyde is fundamental reaction in organic chemistry. widely in used industrial applications such as acetic acid production. processing, and pharmaceuticals. Conventional catalysts, including silverbased (Ag/SiO₂) and copper-based (CuO) materials, exhibit high catalytic efficiency but suffer from drawbacks such as high cost, toxicity, and environmental impact.

Recent advances in green chemistry have highlighted the potential of plant-derived compounds as alternative catalysts. Botanical extracts rich in phenolic compounds and essential oils exhibit redoxactive properties that facilitate oxidation reactions. While plant extracts have been extensively studied for antimicrobial and antioxidant properties, their catalytic applications in organic synthesis remain underexplored.

This study aims to bridge this gap by evaluating the efficiency of Mentha spicata and Thymus vulgaris extracts as catalysts for ethanol oxidation. The proposed mechanism involves the redox-active

phenolic compounds in the extracts facilitating the oxidation of ethanol to acetaldehyde. Additionally, the catalytic performance of these extracts is systematically compared to traditional metal catalysts to assess their industrial viability.

Materials and Methods

1. Plant Extract Preparation

Materials: Fresh Mentha spicata leaves, dried Thymus vulgaris (20 g each), ethanol (100 mL, 99% purity)

Procedure:

- 1. Grind plant material into fine powder.
- 2. Soak in ethanol for 24 h with periodic stirring.
- 3. Filter through Whatman No. 1 paper.
- 4. Concentrate the filtrate using rotary evaporation (40°C, 100 mbar).

2. Catalytic Oxidation of Ethanol

Reagents: Ethanol (10 mL, 99%), hydrogen peroxide (2 mL, 3%), plant extract (1 mL), metal catalysts (Ag/SiO₂, CuO, 50 mg).

Procedure:

- 1. Mix ethanol, H_2O_2 , and plant extract in a conical flask.
- 2. Heat at 50°C for 30 min under constant stirring.

Analyze the product using GC-MS.

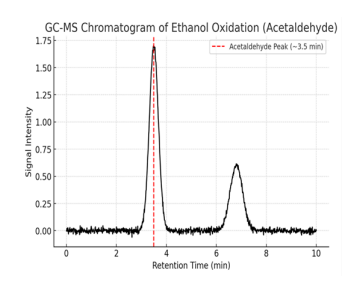


Figure 1. GC-MS chromatogram showing acetaldehyde formation

3. Analytical and Characterization Techniques

- **GC-MS: Column**: HP-5MS (30 m × 0.25 mm); carrier gas: helium; temperature program: 40°C (2 min) to 250°C (10°C/min).
- Scanning Electron Microscopy (SEM):
 Used to analyze the surface morphology of plant-based and metal catalysts.
- Thermogravimetric Analysis (TGA): Conducted from 30°C to 600°C to assess catalyst stability.
- Kinetic Analysis: Reaction rates were determined at varying temperatures (30–70°C) to estimate activation energy using the Arrhenius equation.

Results and Discussion

Catalytic Performance Comparison

Catalyst	Conversion (%)	Activation Energy (kJ/mol)	Stability (TGA Residue, %)
Mint extract	68.2 ± 2.5	42.7	85.6
Thyme extract	54.7 ± 3.1	47.1	78.2
CuO	72.5 ± 1.8	40.3	92.4
Ag/SiO₂	81.3 ± 1.2	38.5	95.8
No catalyst	<5		52

Figure 2. SEM images comparing the surface morphology of CuO and plant-based catalysts.

Kinetics and Activation Energy

Kinetic studies revealed that plant-based catalysts have activation energies slightly higher than CuO and Ag/SiO₂ but still within a practical range for industrial applications.

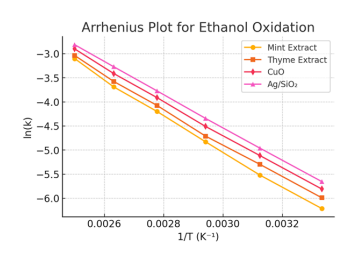


Figure 3. Arrhenius plot showing activation energies of different catalysts.

Thermal Stability and Reusability

- **TGA Analysis**: Mint extract retained 85.6% mass at 500°C, indicating moderate thermal stability.
- Reusability: Catalysts were tested for three consecutive cycles, with mint extract maintaining ~90% efficiency after the third cycle.

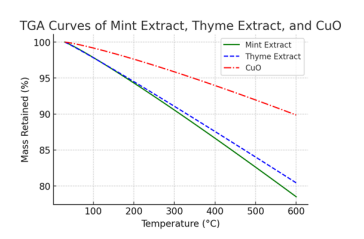


Figure 4. TGA curves of mint extract, thyme extract, and CuO.

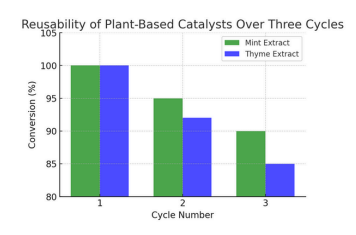


Figure 5. Reusability of plant-based catalysts over three cycles.

Conclusion

This study demonstrates that Mentha spicata and Thymus vulgaris extracts serve as effective green catalysts for ethanol oxidation, with performance comparable to CuO. Kinetic and stability analyses confirm their viability as sustainable alternatives. Future research should explore large-scale applications and optimization strategies to further enhance efficiency.

References

- 1. Clark, J. H.; Macquarrie, D. J. Handbook of Green Chemistry and Technology; Blackwell Science: Oxford, 2002.
- 2. Sheldon, R. A.; Arends, I. W. C. E.; Hanefeld, U. Green Chemistry and Catalysis; Wiley-VCH: Weinheim, 2007.
- 3. Anastas, P. T.; Warner, J. C. Green Chemistry: Theory and Practice; Oxford University Press: New York, 1998.
- 4. Zhang, X.; Wang, Y.; Li, Q. Catalytic Oxidation of Ethanol to Acetaldehyde over Metal Oxide Catalysts; Journal of Catalysis, 2015, 330, 135-144.
- 5. Liu, H.; Iglesia, E. Selective Oxidation of Ethanol to Acetaldehyde on Vanadium Oxide Catalysts; Journal of Physical Chemistry B, 2003, 107 (40), 10840-10847.
- 6. Chemat, F.; Vian, M. A.; Cravotto, G. Green Extraction of Natural Products: Concept and Principles; International Journal of Molecular Sciences, 2012, 13 (7), 8615-8627.
- 7. Li, Y.; Yang, D. J.; Chen, S. L. Plant Extracts as Green Catalysts for Organic Synthesis; Green Chemistry, 2018, 20 (5), 1042-1054.

Author

Dr. Saad Althubyani is an educational expert holding a Ph.D. in Educational Foundations, with extensive experience in educational supervision and the management of educational projects. He has contributed to the development of training programs and innovative

educational packages aimed at improving educational performance. He is distinguished by his leadership skills, strategic planning, and the development of sustainable educational solutions. He strives for excellence.

Novel Flash System for Determining Gas-Water Ratio in Reservoir Fluids

Ahmed Sahl*, Abdullah Almousa, Mohammed Bashrawi, Faisal Alissa Aramco, EXPEC ARC, Dhahran, Saudi Arabia *Corresponding author; email: ahmed.sahl@aramco.com

Abstract

The gas-water ratio (GWR) is crucial for understanding reservoir compartmentalization, and connectivity to water sources. This indicator is key during exploration and development operations. A novel gas-water flash separator system was designed to determine the GWR in reservoir fluids. The system is capable of separating pressurized reservoir fluids into gas and water phases at atmospheric conditions, measuring the volume, weight, temperature, and pressure of the liberated gas, while determining the weight and density of the separated water. The system is highly sensitive to low gas concentrations and is designed for use in laboratories and at well sites, providing real-time data for management purposes. system includes a glass trap for phase separation, gasometer gas measurement, and a gas chromatograph for chemical composition analysis. system's ability to capture and analyze trace volumes of gas makes it particularly useful for reservoirs with low gas-water ratios.

Introduction

Conventional hydrocarbons are located in subsurface geological formations of sandstone or carbonate lithologies.

Oil or gas producing wells are drilled inside of the formation to allow for hydrocarbon production. On the other hand, waterinjection wells are drilled beneath the oillevel to ensure oil-lifting and pressure support. In a conventional hydrocarbon production well, gas, oil, and water are produced simultaneously. However, they are produced at different proportions from various depths. Reservoir engineers often rely on indicators obtained from fluid analysis to make decisions such as wellbore depth, and horizontal-section length, and direction.

The accurate determination of gas-water ratios in reservoir fluids is crucial for effective reservoir management. The gaswater ratio (GWR) is defined as the volume of gas produced from a barrel of produced water when cooled and depressurized to standard conditions. This measurement is essential for various exploration and development operations, including drilling fluid composition, hydraulic fracturing, and secondary oil recovery. However, current gas-water ratio testing devices often lack sensitivity to measure low concentrations and are typically located far from well sites, leading to delays in sample analysis and potential contamination.

System Design and Components

A GWR system has been designed to accommodate varying operation conditions to separate reservoir fluids into gas and water phases while accurately measuring the liberated gas volume. The system allows for on-site analysis, reducing the time between sample collection, analysis minimizing the risk of sample and contamination. the gas-water flash separator system consists of several key components as shown in figure 1.

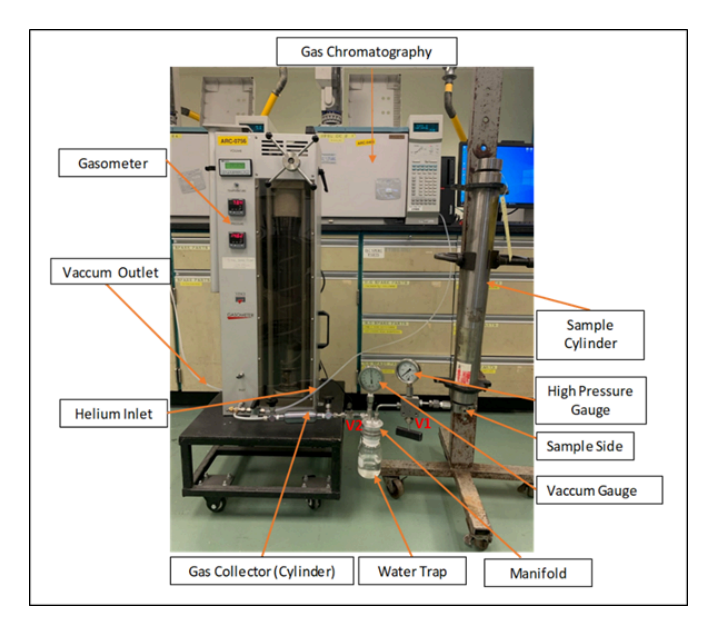


Figure 1. Gas/Water flash separator system for reservoir fluid.

The separator system is a sophisticated apparatus designed to accurately determine the GWR in reservoir fluids. At its core, the system features an inlet water line that connects to a sample cylinder containing pressurized reservoir fluid. This inlet water line facilitates the transfer of the pressurized fluid into the system for further processing. The fluid is then directed into a glass trap, which is sealed with a manifold. The glass trap plays a critical role in the system, as it allows the pressurized reservoir fluid to separate into two distinct phases-flashed gas and

water-when reservoir exposed atmospheric conditions. The use of glass for the trap is essential, as it prevents chemical reactions with reactive components commonly found in reservoir water, such as sulfide. The hvdrogen svstem incorporates gasometer. which is а connected to the glass trap via a gasometer flow line. The gasometer is responsible for measuring the volume, temperature, and pressure of the flashed gas liberated during the separation process. It is equipped with a gas volume meter, a gas temperature gauge, and a gas pressure gauge to ensure precise measurements. To capture and collect the liberated gas, the system includes one or more flashed gas cylinders. These cylinders are fitted with valves at both ends to control the flow of gas and can be easily removed for further analysis using a gas chromatograph. This feature is particularly useful for determining the chemical composition of the flashed gas, which is critical for reservoir management. Additionally, the system includes several safety features, such as a hydrogen sulfide detector, which monitors for toxic gas leaks and ensures the safety of operators during operation.

Methodology

The system can be operated in the following steps sample preparation that includes connecting a pressurized reservoir fluid sample to the inlet water line. Then, the fluid is pressurized to monophasic conditions using a positive displacement pump. After that, water/gas phases are separated in atmospheric conditions which allow water accumulation in the glass trap. Later, gas measurement is carried out through a gasometer, where its volume, temperature, and pressure are measured.

Simultaneously, the weight and density of the separated reservoir water are measured. Finally, the flashed gas is captured in one or more flashed gas cylinders then analyzed using a gas chromatograph to determine the gas composition which allows for calculating the gas-water ratio is by comparing the volume of the flashed gas to the weight and density of the reservoir water.

Results and Discussion

The system was tested using representative sample of reservoir water. The results, as shown in Table 1, include measurements from the gasometer (gas phase data) and the initial and final weight of the glass trap (water phase data). The gas phase data includes the specific gravity of the flashed gas, and the water phase data includes the density of the obtained water phase. The gas-water ratio was calculated to be 2 standard cubic feet per barrel (SCF/bbl).

Table 1. Gas/Water flash separator results

Component	Mol%
Nitrogen	1.27
Carbon Dioxide	1.80
Hydrogen Sulfide	0.00
Methane	83.54
Ethane	9.46
Propane	2.69
i-Butane	0.40
n-Butane	0.56
i-Pentane	0.15
n-Pentane	0.09
Hexanes	0.03
Heptanes	0.01
Octanes	0.00
Nonanes	0.00
Decanes	0.00
Total	100.00

The gas chromatograph analysis of the flashed gas revealed the presence of various compounds, including nitrogen, carbon dioxide, hydrogen sulfide, and methane. The results demonstrate the system's ability to accurately measure low gas concentrations and provide detailed chemical composition analysis.

Conclusion

The gas-water flash separator system presented in this paper offers a significant advancement in the determination of gaswater ratios in reservoir fluids. sensitivity to low gas concentrations and ability to provide real-time data make it an invaluable tool for reservoir management. The system's design ensures accurate and reliable measurements, even in remote locations, and its safety features protect operators from potential hazards. Future work will focus on further optimizing the system for use in a wider range of reservoir conditions and integrating additional analytical capabilities.

References

- 1. Schön, J. H. (2011). Physical properties of rocks: A workbook (Vol. 8). Elsevier.
- 2. Sahl, A. M., Almousa, A. F., Bashrawi, M. H., & Sequeira, D. S. (2024). System and Method for Determining Gas-Water Ratio in a Reservoir Fluid. U.S. Patent Application No. US 2024/0201150 A1.
- 3. Mohammad Ibrahim Al-EidEmmanuel C. UbaMohammed Sajjad Ali (2012). Fluid compositional analysis by combined gas chromatographic and direct flash methods Application No. US2012/0085149A1.

Authors

Ahmed M. Sahl is the dedicated Lab Manager of the Advanced Materials Lab, renowned for overseeing various sections and upholding the highest safety standards. With a structured approach to tasks.

Faisal M. Alissa is a researcher in oilfield chemistry at KAUST Upstream Research Center. His work focuses on flow assurance, water management, and wellbore stimulation. Faisal's scientific and operational contributions have resulted in 6 granted patents, and 7 papers within 5 years in the industry.

Abdullah F. Almousa is a skilled Lab Technician in the Fluid Composition Analysis section of the Hydrocarbon Phase Behavior Unit. With a keen eye for detail and a commitment to precision, Abdullah ensures accurate and reliable analysis, contributing to the lab's success.

Mohammed H. Bashrawi is a proficient Lab Technician in the Fluid Composition Analysis section of the Hydrocarbon Phase Behavior Unit. His dedication to maintaining high standards and delivering precise results plays a vital role in the lab's operations.

Place Your Advertisement Here

Contact us at editorial@cris.org.sa

A Lab-based case study of root cause analysis of filter sludge deposits from natural gas liquid recovery plants and quantitative phase analysis by Rietveld method

Muthukumar Nagu*, Husin Sitepu¹ Wala A. Algozeeb, Nayef M Alanazi Aramco, Research and Development Center, Dhahran, Saudi Arabia * Corresponding author; email: muthukumar.nagu@aramco.com

Abstract

Unknown and complex sludge deposits that are frequently accumulated inside refinery and gas plants' equipment — can cause failures and temporarily shut down refineries and gas oil separation plants. Therefore, when these particular generated sludge deposits arrived at the laboratory, the authors firstly conducted the sample preparation with a great care to obtain the best possible data. In this article, the carefully separated authors nonhydrocarbon (i.e., crystalline inorganic materials or insoluble part) from the hydrocarbon part (i.e., dichloromethane soluble) of the sludge deposits. Subsequently, the X-ray powder diffraction (XRD) data of the inorganic crystalline materials part of the sludge deposits were measured and identified; and Rietveld method was used to quantify for each of the identified phases. Additionally, the ranges of the hydrocarbons of the dichloromethane soluble part were screened by using the gas chromatography mass-spectrometry (GC-MS). Thermogravimetric analysis (TGA) used to determine the contents (wt%) of the organic and inorganic crystalline materials. Environmental scanning electron microscopy of the energy-dispersive X-ray Spectrometry (ESEM/EDX) was used to

measure the elements appeared on the samples. The TGA results revealed that the sludge deposits from the bottom dehvdration unit filters (sample A) contained pf 86 wt% of organics and 14 wt% of inorganic crystalline compounds and. Also. the presence of (methyldiethanolamine MDEA piperazine), elemental sulfur and C_9-C_{25} hydrocarbon in Sample-A. In this paper, advanced materials characterization results of the all sludge deposit samples from different NGL Recovery Unit locations were discussed. The findings support the field engineers at the gas plant to overcome the problems of the affected equipment by drawing up the right procedures and taking preventive action to stop the generation of those particular sludge deposits.

Introduction

Smith [1] and Khanfar and Sitepu [2] described that the sludge frequently accumulated inside refineries and gas plants' equipment, and caused failures and temporarily shut operations. Subsequently, Sitepu and Zaidi [3] developed the new method in sample preparation to separate the nonhydrocarbon part (i.e., crystalline

inorganic materials) from the hydrocarbon part (i.e., dichloromethane soluble) of the sludge deposits. They described three types of the procedures in order to obtain the best possible XRD data of the small amounts of crystalline materials part of the sludge deposits, and therefore, the XRD data can be accurately identified by the combined High Score Plus software and International Center for Diffraction Data (ICDD) and Powder Diffraction File (PDF-4+) database [4-7] and yielded the reproducible results. For example, when the

- water-based sludge deposits were received from the oil field operations, a known quantity of deposit was put into a beaker - and dried these deposits in a fume hood between 2 and 3 days.
- unknown deposits were from the sulfur products, the XRD data of these deposits should be measured without pretreatment, and
- oil-based sludge deposits from refineries and gas plants were received, these sludge deposits were subsequently treated with dichloromethane (DCM), and filtered in the filtration assembly to separate the dichloromethane insoluble part (i.e., inorganic materials or non-hydrocarbon from the dichloromethane soluble part (i.e., hydrocarbon). Note that,
 - the dichloromethane insoluble part, i.e., inorganic materials or nonhydrocarbon, was mounted into the diffraction X-ray powder diffractometer's holder, sample measured the X-ray powder diffraction (XRD) data, identified the XRD data by the combined High Score Plus software and ICDD-PDF-4+, and quantified all the identified phases by the Rietveld method; and

 the dichloromethane soluble part, i.e., hydrocarbon, was screened by gas chromatography mass spectrometry (GC-MS) to determine the range of the hydrocarbon part of the sludge deposits.

The challenges and novel of this paper were to extend the work of Sitepu and Zaidi [3] if the phase identification results of the XRD data of the small amounts of crystalline inorganic materials part of the sludge deposits by the combined High Score Plus software and International Center for Diffraction Data (ICDD) and Powder Diffraction File (PDF-4+) database [4-7] can be accurately obtained and the results are reproducible. Subsequently, quantitative phase analysis for all of the identified phases was conducted by the advanced Rietveld method with the March model for the correction of intensities due to the of crystallographic preferred orientation [8-9] (i.e., texture of crystalline materials).

These accurate and reproducible X-ray powder diffraction data and Rietveld quantitative phase analysis results can guide the oil field engineers at the natural gas liquid (NGL) recovery unit to overcome the problems of the affected equipment by drawing up the right procedures and taking preventive action to stop the generation of those particular deposits. Noted that those particular deposits accumulated at the NGL recovery units (e.g., feed gas filters, booster pump inlets, and heat exchangers). The NGL recovery units consists of a dehydration unit, mercury removal unit, amine unit and brazed aluminum heat exchangers - BAHEs, and therefore when the natural gases pass through these units it will be purified by

removing the acidic gases (for example., CO_2 and H_2S), moisture and Mercury, see Figure 1.

NOL Feed from acid gas children

Feed gas children

Sample C

Sample BMG

Sample BMG

Fallers

Sample BMG

Fallers

Fall

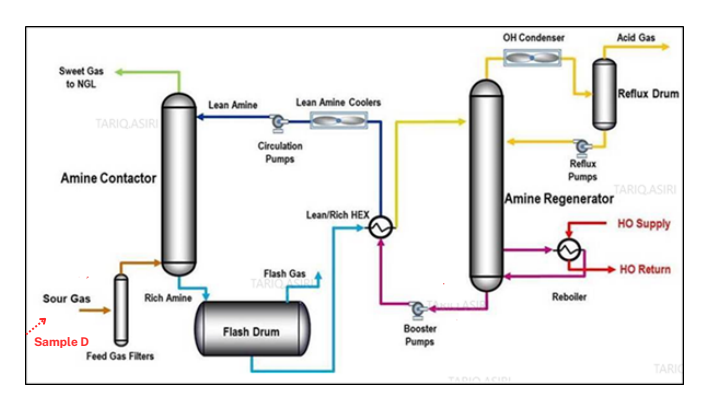


Figure 1. The schematics of the NGL recovery units {(i) A, B, C samples location from dehydration and mercury removal units (ii) D and E samples from acid gas removal unit)}, where the sludge deposits were accumulated and collected.

The blockage of deposits on the filters might be occurred due to the formation of corrosion products, catalyst materials, some organic compounds from previous unit in NGL recovery plants. Therefore, it is very important to identify the nature and source of the XRD data of deposits by using the High Score Plus software (X'Pert High Score Plus Version 3.0e PANalytical Inc.) [10], combined with the International Powder Diffraction Data (ICDD) of the powder diffraction file (PDF-4+) database [11] of the standard reference materials. Additionally, the authors provide the findings and support to the plant engineers, to take proper action to prevent future occurrences, thereby avoiding a plant

slowdown that could result in loss of production.

The main objective of the present study was examine the phase identification inorganic materials (non-soluble or nonhydrocarbon) found in different pieces of equipment at NGL recovery plants using the High Score Plus software. Once all the phases for each of the unknown inorganic deposits' XRD data had successfully been identified using the High Score Plus software, then the quantitative phase analysis of XRD data for each of the identified phases was determined by using the Rietveld method with the March model for the crystallographic preferred orientation correction [8-9]. The findings will help NGL plant engineers take proper action to prevent future occurrences [1-7]. The other objectives of this article were to measure the organic and inorganic contents of the as-received sludge deposits by TGA analysis; and screen the range of the hydrocarbon part of the sludge deposits by GC-MS. Additionally. the authors determined the nature. source and formation mechanism of deposits formed in the NGL recovery units.

Experimental Procedure

The description of the as-received sludge deposits from NGL Recovery Unit (A, to E), which were investigated in this study, is depicted in Table 1. The spectroscopy techniques used in this study were thermogravimetric analysis (TGA) to measure the organic and inorganic contents (see Section 2.1.1), Gas Chromatography Mass Spectrometry (GC-MS) to screen the ranges of the hydrocarbon of the sludge deposits part (i.e., dichloromethane soluble part) - see Section 2.1.2 below, and

Environmental Scanning Electron Microscopy Energy Dispersive spectrum (ESEM-EDS) techniques to detect the elements appear at the unknown and complex deposits (Samples A to E), see Section 2.1.3 below. . Finally, X-Ray Powder Diffraction (XRD) data and Rietveld method were employed to perform quantitative analysis of the inorganic crystalline materials part of the sludge deposits, see Section 2.2 below for details. Therefore, the characterization of the sludge deposits independently obtained from spectroscopy and diffraction techniques can support to overcome the problems by drawing up the right procedures and taking preventive action to stop the generation of those particular deposits.

Table 1. Sample description of the deposits investigated in this study

Sl. No	Service	Location	Samples
1	Liquid Hydrocarbon	Inlet strainer	А
2	Dry Sweet Gas	Inlet nozzles of multiple BAHEs	В
3	Dry Sweet Gas	Upstream dust filter	С
4	Dry Rich Gas	Feed gas filters inlet	D
5	Lean Amine	Amine unit regenerator booster pump inlet	Е

Analytical Methods

Spectrometry

Thermogravimetric analysis (TGA): The asreceived sample was analyzed using TGA Q500 (TA) Thermogravimetric Analyzer that was programmed at a heating rate of 20 °C/min between 25 °C to 900 °C under air. The aim of this analysis was to determine the weight losses and the organic/inorganic content.

Gas chromatography mass spectrometry (GC-MS) analysis for organic composition (i.e., hydrocarbon or soluble part): A gas chromatograph equipped with a Mass and spectrometer non-polar а chromatographic column (DB1, 0.25mm ID and 120m long) was used. The GC oven was ramped from 30 °C to 300 °C at 5 °C/min. The sample was extracted dichloromethane and then injected into the instrument. For identification purposes, the collected spectra were matched with NIST mass spectra database.

Environmental scanning electron microscopy (ESEM) with the energy dispersive spectrometry (EDS) analysis: The samples were mounted on aluminum stub holders using double-sided carbon tape, and then were inserted into the ESEM sample chamber. The ESEM was operated at 20 kV, low pressure mode and 9-10mm working distance.

Diffraction

2.2.1. Qualitative Analysis, and Quantitative Phase Analysis of Whole-Patterns X-ray Powder Diffraction by Rietveld Method. For Qualitative Analysis, which is also called either Chemical Analysis, or Phase Identification, or Finger Print of X-ray powder diffraction (XRD) data, ICDD (2018 and the references therein) [11] described that the International Centre for Diffraction Data (ICDD) of the Powder Diffraction File (PDF) database has the primary purpose to

- world-widely serve as a quality reference tool for the powder diffraction community including Labbase X-ray powder diffraction, and large facilities (synchrotron and neutron powder diffraction data) and
- edit, publish, and distribute of XRD data for the identification of materials (i.e., 450,000+ crystallographic information files are available at the 2022 version of the ICDD-PDF-4+ database including 76 of them are the crystallographic information files from the work of one of the authors (HS)).

The ICDD-PDF+4 database consists of the crystallographic information files (CIFs) of crystalline materials that can be used to determine phase identification of X-ray, synchrotron, and neutron powder diffraction data. Moreover, the PDF has been the primary qualitative crystalline phase identification reference for powder diffraction data: and the ICDD-PDF database has been extended to semicrystalline and amorphous (non-crystalline) materials [11]. The ICDD-PDF database provides the details of crystal structure of crystalline materials (e.g. space group, lattice parameters, atomic coordinates, and thermal parameters) which can be used to perform phase identification, quantitative phase analysis by Rietveld method [12-16], crystallographic preferred orientation characterization [8-9,17] and determination [18], and crystal structure refinement by Rietveld method [7-9]. ICDD [11] indicated that the ICDD-PDF database and other crystallographic databases are one of the key tools to perform structure refinements in the International of Crystallography (IUCr) Powder Diffraction Community; and ICDD-PDF-4+ highlighted that the crystallographic database

- a. consists of structure details and provide the PDF card for the inorganic and organic diffraction data used for phase identification and materials characterization by X-ray, synchrotron, and neutron powder diffraction data;
- b. is editorially reviewed and processed according to the ISO 9001:2015, and therefore, this crystallographic database is certified; and
- c. evolves both computer and web accessible, serves a wide range of disciplines covering academic, industrial, and government laboratories, and describes in details the content of database entries are presented to enhance the use of the PDF.

For XRD data measurements, the asreceived deposits were manually ground by an agate mortar and a pestle for several minutes to achieve a fine particle size [8-9,17]. Then, the fine powders were mounted into the sample holders of the XRD by backpressing. To perform the chemical analysis in this study, the authors used the High Score Plus software [10] and combined with the International Powder Diffraction Data (ICDD, 2018) [11] of the powder diffraction file (PDF-4+) database of the standard reference materials, which is an excellent analytical technique used for the phase identification of XRD data [2-7, 19-21]. Importantly, the phase identification of XRD data of the very small of the crystalline inorganic part materials can accurately be used to differentiate between different forms of a calcium carbonate (CaCO₃) scale formation materials either in the form of calcite or scale deposits (aragonite) or vaterite that have different structure [2]. Additionally, the iron sulfide corrosion products that are appeared the very small quantities of the crystalline

inorganic part materials of the sludge deposits have a wide range of chemical compositions and different crystalline structures; for example, marcasite has an orthorhombic crystal structure, greigite has a cubic crystal structure, and mackinawite has a tetragonal crystal structure.

Quantitative phase analysis [12-16] or phase composition or wt% (W_p) for each of the identified phases (p) is proportional to the product of the scale factor (s) as derived in the Rietveld refinement, with the mass and volume of the unit cell according to:

$$W_p = s_p(ZMV)_p / \sum_{i=1}^n s_i(ZMV)_i$$

where Z is the number of formula units per unit cell, M is the mass of the formula unit and V is the unit-cell volume (in \mathring{A}^3), respectively. The advantages of this quantitative phase analysis by Rietveld method [9-16] compared to the conventional reference intensity ratio method are that quantitative phase analysis by Rietveld method provides

- accurate and precise results without the need for complex procedures of laborious experimental calibration,
- 30,000 times quicker than the reference intensity ratio method,
- standard less
- all reflections in the pattern are explicitly included, irrespective of overlap
- the background is better defined since a continuous function is fitted to the whole-pattern XRD data,
- the preferred orientation effects can be corrected and determined, and
- the crystal structural and peak-profile parameter scan can be refined as part of the same analysis.

Reproducibility of XRD Phase Identification and Quantifications by Rietveld Method.

Micro-absorption, which is the presence of absorption contrast between phases, is one of the main sources of error to perform accurately quantitative phase analysis of high quality of high-resolution XRD data by Rietveld method (Scarlett et al. 2006 [16]; and the references therein) described that is. They showed that the micro-absorption proves to be challenging in some circumstances of the quantitative phase analysis by Rietveld method. To achieve fine particle size [8-9] and eliminate microabsorption effects, the limited amount of inorganics deposits or the non-hydrocarbon parts were manually ground by the authors in an agate mortar and a pestle with a great care for several minutes. Subsequently, the authors reproduced the results by carefully repeating the sample preparations. Note that in order to achieve inadequate intensity reproducibility [8-9] the size distribution of the limited amount of inorganic crystalline materials part of the sludge deposits were modified by McCrone micronizing mill following the techniques described by O'Connor, Li and Sitepu (1991) [17] and Sitepu, O'Connor and Li (2005) Excellent agreement was obtained between the results of the two experiments McCrone mill-micronizing - and manually ground in an agate mortar and a pestle technique; and following to O'Connor, Li and [17] the micro-absorption Sitepu correction was not conducted - in the Rietveld refinement. The results of the manually ground in an agate mortar and a pestle for several minutes are quoted in this article as the experimental data of the limited amount of inorganics crystalline

materials part of the sludge deposits were superior quality in terms of counting statistics.

Results and Discussions

The as-received sludge deposits were analyzed by TGA to get an insight about the total weight loss and the residual mass, and subsequently the GC-MS was implemented for the organic extractable by dichloromethane in the sample or the hydrocarbon or soluble part. Moreover, ESEM/EDS (i.e., low resolution, high intensity and high background) was used to detect the elements appeared on the samples due to the facts that the samples were limited amounts for WDXRF analysis (i.e. a high-resolution, low intensity, background and high background ratio). Finally, the phase identification and quantitative phase analysis of the small quantity of the inorganic crystalline materials part of the sample or the non-soluble part or nonhydrocarbon was subsequently performed by XRD data and Rietveld method.

TGA Results: Based on TGA analysis (Figures 2 and 3), the as-received five samples showed that the contents of organic and inorganic crystalline materials are 87 wt% and 13 wt% for Sample-A, 11 wt% and 89% for Sample-B, 14 wt% and 86 wt% for Sample-C from NGL Recovery Unit. The corresponding values are 26 wt% and 74 wt% for Sample-D and 77 wt% and 23 wt% for Sample-E from Amine Unit. From TGA data, Sample A and Sample E contains more organic materials than inorganic compounds.



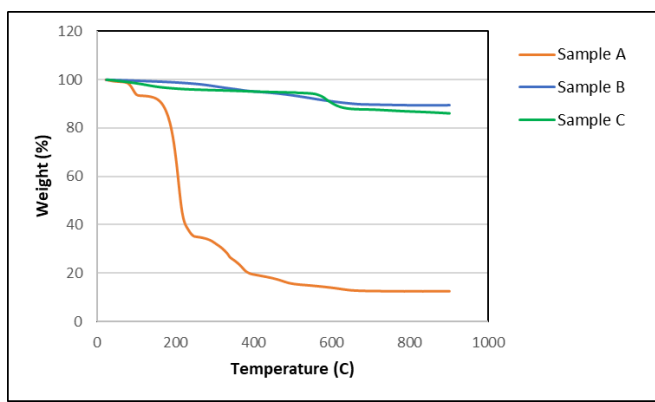
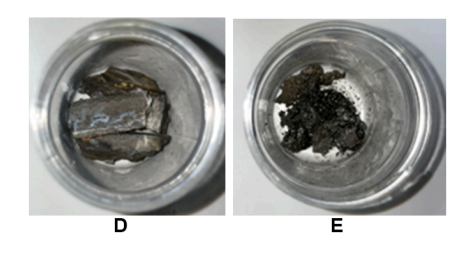


Figure 2. TGA thermogram for the samples A, B and C and their photos from NGL Recovery Unit.



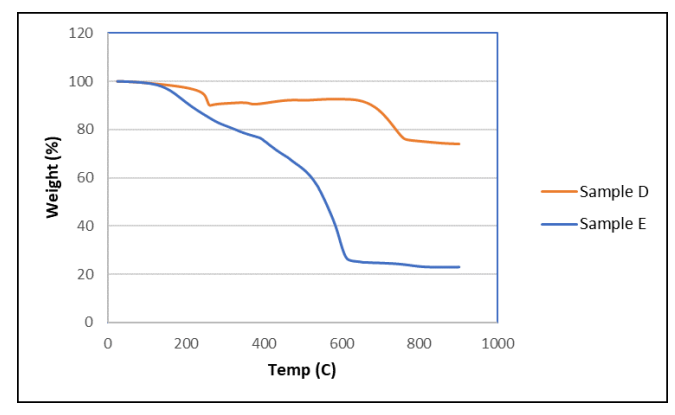
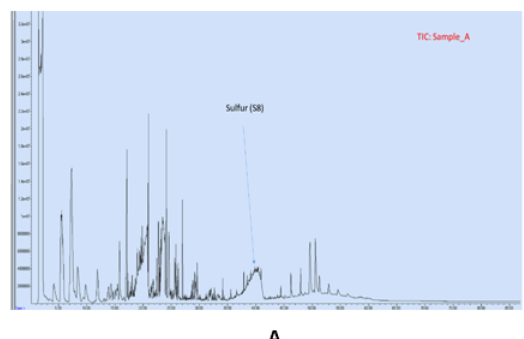
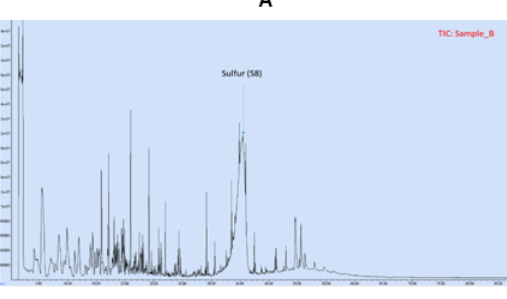


Figure 3. TGA thermogram for the samples D and E and their photos from Amine Unit.

GC-MS Results: For the GC-MS screening, extractions from sample was obtained using dichloromethane or the hydrocarbon or soluble part. The obtained chromatograms with identified organic compounds are depicted from Figures 4 and 5.





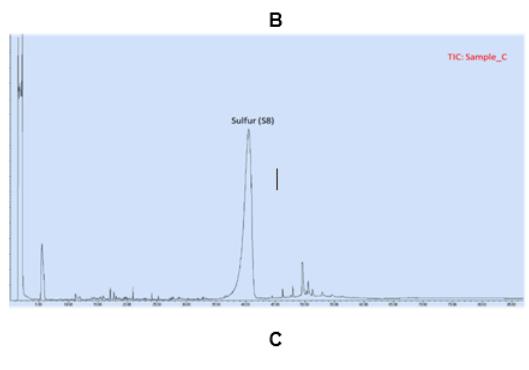
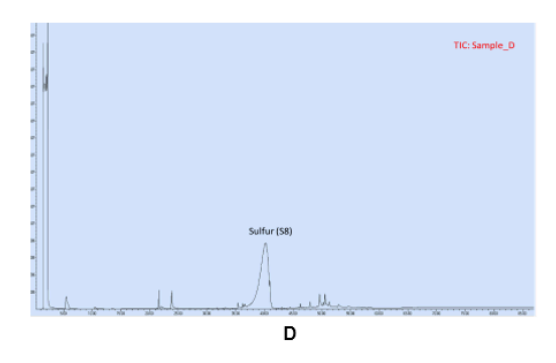


Figure 4. Gas chromatography (GC-MS) chromatogram (TIC) of the samples A, B and C from NGL recovery unit



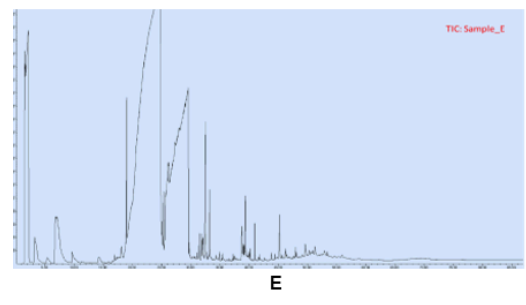


Figure 5. Gas chromatography (GC-MS) chromatogram (TIC) of the samples D and E from Amine unit

- For Sample-A from NGL recovery unit, the result indicates the present of alkane C₉-C₂₅₊ and Elemental Sulfur (S₈).
 In addition to Triethylene glycol, Methyldiethanolamine (MDEA),
 Piperazine, 1-methyl- and other unidentified organic compounds.
- For Sample-B from NGL recovery unit, the result indicates the present of alkane C₉-C₂₅₊ and Elemental Sulfur (S₈).
 In addition to Butyl glycol and other unidentified organic compounds.
- For Sample-C from NGL recovery unit, the result indicates the present of alkane traces of C_9 C_{25} . In addition to, Elemental Sulfur (S₈), Butyl glycol and other unidentified organic compounds.
- For Sample-D from Amine Unit, the result indicates the present of suspected alkane traces of C₂₀ - C₂₅. In addition to, Elemental Sulfur (S₈), 1,4-Dioxan-2-ol, Diethylene glycol, Triethylene glycol and other unidentified organic compounds.
- For Sample-E from Amine Unit, the result indicates the present suspected alkane traces of C_{20} - C_{25} . In addition to. Piperazine, Methyldiethanolamine (MDEA), other Triethylene glycol and unidentified organic compounds.

In amine unit, methyldiethanolamine (MDEA) and piperazine are added to remove the acid gases (H_2S & CO_2) and theses amines could be escaped from the amine unit and reaching to downstream dehydration unit.

Quantitative phase Analysis Results obtained from XRD Data and Rietveld Method: One of the challenges in phase identification of XRD data of the crystalline

materials is to determine the minor and/or trace phases appear on the samples, whereas the major phases usually can be determined by the X-ray scientists. Note that, those the minor and/or trace phases significantly important for the field engineers to determine the root-cause and source and the best prevention method to avoid the generation of those particular deposits. Figures 6 and 7 show the XRD phase and composition identification results of the small quantity of inorganic crystalline phases or the non-soluble or non-hydrocarbon part of the five samples. It can be seen from Figures 6 - 9 that the samples from

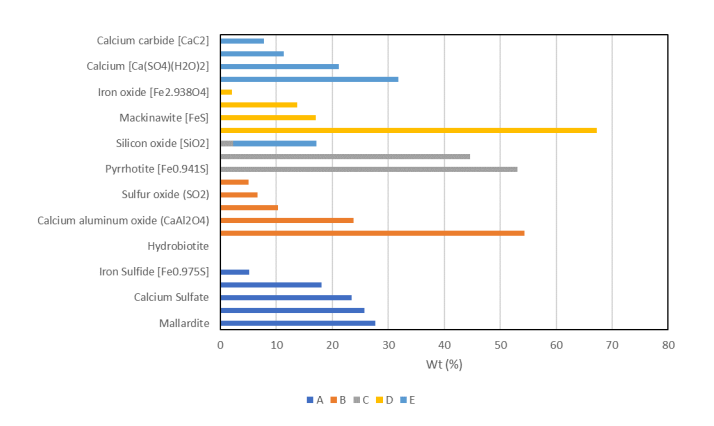


Figure 6. Summary of the XRD Phase Composition Results for all the Identified Phases Obtained from Reference Intensity Ratio Method.

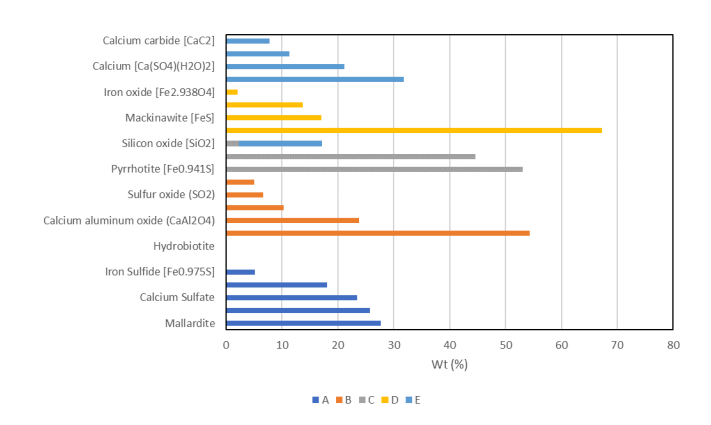


Figure 7. Summary of the Elements Detected by ESEM/ EDS and Its Concentration (wt%) Semi-quantitatively Obtained from Its Software.

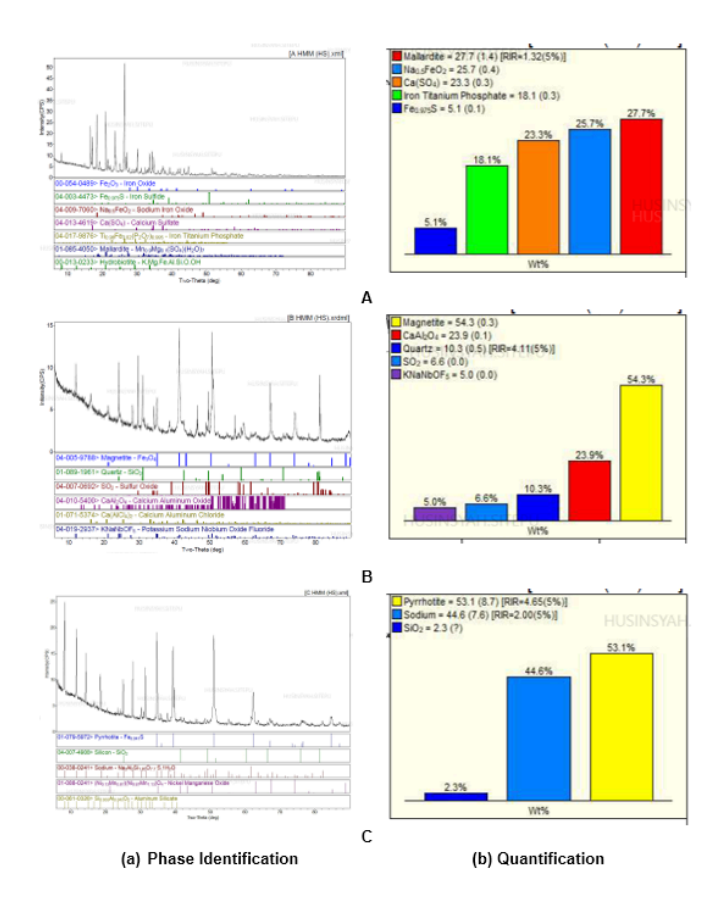


Figure 8. Phase Identification results of the XRD data of Samples A, B and C from NGL recovery unit obtained from the combined High Score Plus software and the powder diffraction file (PDF-4+) database of International Center for Diffraction Data (ICDD).

NGL Recovery Unit consists of

- $^{\circ}$ 27.7 wt% of mallardite $[Mn_{0.9}Mg_{0.1}(SO_4)(H_2O)_7,\ 25.7$ wt% of sodium iron oxide $(Na_{0.5}FeO_2),\ 23.4$ wt% of calcium sulfate $(CaSO_4),\ 18.1$ wt% of iron titanium phosphate $[Ti_{0.98}Fe_{0.02}(P_2O_7)_{0.995}],\ 5.1$ wt% of iron sulfide $[Fe_{0.975}S]$ with the traces of iron oxide $[Fe_2O_3]$ and hydrobiotite [KMgFeAlSiOOH] for Sample-A; see Figures 6 8.
- 54.3 wt% of iron oxide corrosion product in the forms of magnetite [Fe₃O₄], 23.8 wt% of calcium aluminum oxide (CaAl₂O₄), 10.3 wt% of quartz (SiO₂), 6.6 wt% of sulfur oxide (SO₂) and 5.0 wt% of

potassium sodium niobium oxide fluoride [KNaNbOF $_5$] with the trace of calcium aluminum chloride [Ca(AlCl $_4$) $_2$] for Sample-B; see Figures 6–8.

• 53.1 wt% iron sulfide corrosion product in the form of pyrrhotite [Fe_{0.941}S], 44.6 wt% of sodium [Na₂Al₂Si_{1.85}O_{7.75}H₂O], 2.3 wt% of silicon oxide [SiO₂] with traces of nickel manganese oxide (Ni_{0.13}Mn_{0.87}) (Ni_{0.87}Mn_{1.13})O₄ and aluminum silicate [Si_{0.955}Al_{0.045}O₂] for Sample-C; see Figures 6 - 8.

Amine Unit consist of

- · 67.3 wt% of sodium calcium magnesium iron silicate $[Na_{0.64}Ca_{0.36}Mg_{0.32}Fe_{0.68}Si_2O_6),$ 30.7 wt% iron sulfide corrosion product in the forms of 17.0 wt% mackinawite [FeS] and 13.7 wt% of greigeite [Fe₃S₄] and 2.0 wt% iron oxide corrosion product [Fe_{2,938}O₄] with the trace of hematite [Fe₂O₃] for Sample-D, see Figures 6 -9; and
- 31.8 wt% of calcium magnesium iron $[Ca_{0.91}Mg_{0.06}Fe_{0.03}(CO_3)],$ carbonate 21.2 wt % of calcium $[Ca(SO_4)(H_2O)_2]$, 14.9 wt% of silicon oxide (SiO₂), 13 wt% of quartz, 11.3 wt% of calcium $[CaMg(CO_3)_2]$ and 7.8 wt% of calcium carbide [CaC₂] with the aluminum trace of silicate $[AlSi_{0.5}O_{2.5}]$ for Sample-E, see Figures 6 - 9.

The sample-C showed the presence of sodium aluminium silicate ($Na_2Al_2Si_{1.85}O_{7.75}H_2O$) and silicon oxide (SiO_2). It might be due to the desiccant materials (ceramic ball contains Al_2O_3 and

SiO₂, Na₂O, K₂O, CaO and MgO) were crushed and escaped from the dehydration unit. The XRD phase composition results are supported by ESEM/EDS results, see Figures 8 and 9. Knowing the phases were involved in the deposits can guide the engineers at the gas plants to overcome the problems by drawing up the right procedures and taking preventive action to stop the generation of those particular deposits.

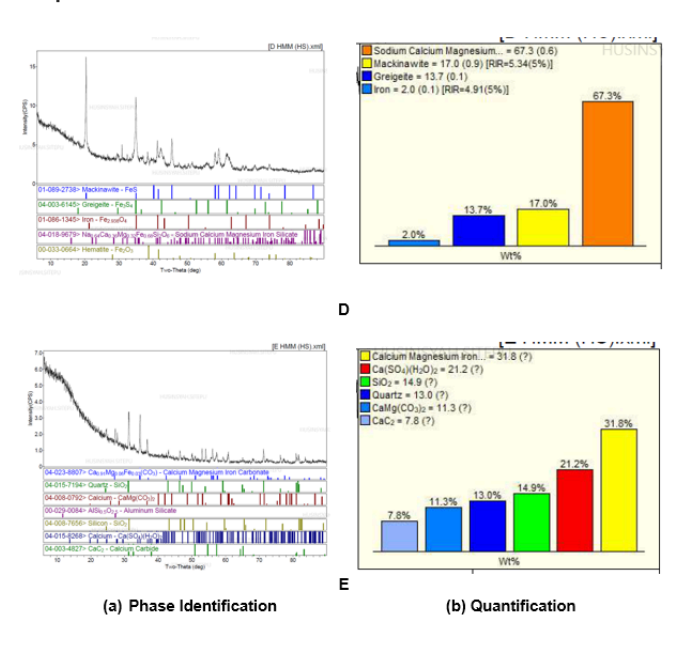


Figure 9. Phase Identification results of the XRD data of Samples D and E from Amine Unit obtained from the combined High Score Plus software and the powder diffraction file (PDF-4+) database of International Center for Diffraction Data (ICDD).

Root Cause Analysis: In NGL Recovery Unit, the sample C showed the 50.0% of desiccant materials (sodium aluminium silicate-Na₂Al₂Si_{1.85}O_{7.75}H₂O and silicon oxide-SiO₂) and 50.0% of corrosion products in the form of iron sulfide (FeS). Iron sulfide corrosion product in the form of pyrrhotite (Fe_{0.941}S) formation was found in the Sample-C. Also, in Amine Unit, Sample-D showed the presence of different forms of iron sulfide corrosion products (mackinawite-FeS and greigite-Fe₃S₄). From GC-MS analysis, elemental sulfur (S₈) formation was confirmed in all samples from NGL dehydration and mercury removal units (A, B, C) and Sample-D from Amine Unit.

The iron sulfide corrosion products (FeS) deposit formation might be due to the dissociation of hydrogen sulfide (H₂S) to elemental sulfur (S_8) . produce dissociated elemental sulfur starts to deposit in the form of small particles that adheres to the internal surface of pipe system. Elemental sulfur, naturally, act as a cathode to the steel pipe due the difference in their potential. An active electrochemical cell will be established as soon as free water or conductive condensates pass over the deposited elemental sulfur particle [22-261.

Smith et al. [27] described that the dry solid sulfur does not produce corrosion of carbon steel. It is only when moisture is present that sulfur induces corrosion [19-25]. In addition, pH of the solution, temperature and presence of chlorides are significant contributors to the corrosion of steels in Scontaining environments [22-28]. Ho-Chung-Qui et al. [28] found the same sequence of corrosion products and severe pitting in flowlines that carried H₂S with water. Temperature plays major role on sulfur corrosion reaction through sulfur hydrolysis [26]. Natural gas liquid (NGL) gathering pipeline corrosion and its failure accidents caused by the corrosive species have been widely reported in the literature [29-33]. The corrosion reactions in presence of elemental sulfur are as follow:

$$S_8 + 8H_2O \rightarrow H_2SO_4 + 6 H_2S$$

$$Fe_{(s)} \rightarrow Fe^{2+}_{(aq)} + 2e^{-1}$$

Reduction:

Oxidation:

$$S_{(s)}$$
 + $2e^{-}$ \rightarrow $S^{2-}_{(aq)}$

Overall:

$$Fe^{2+} + S^{2-} \rightarrow FeS_{(S)}$$

It can be highlighted from the results that the deposits on the filters and feed pumps consist of

- 1.corrosion products as elemental sulfur and different forms of iron sulfide
- 2.desiccant materials as aluminum silicates
- 3. previous unit chemicals e.g., MDEA and Piperazine escaped from amine unit and it was found in the dehydration unit bottom filters.

Conclusion

The present study, a sequence of the lab-based case study using the advanced analytical instruments and techniques was carried out to investigate the deposits in NGL Recovery Units, such as dehydration, mercury removal and acid gas removal units using the spectroscopy techniques (i.e., TGA, GC-MS, ESEM/EDS) and diffraction techniques (XRD data and Rietveld method). Based on the lab analysis data, the following observations has been made from the NGL Recovery Unit (Sample-A, Sample-B and Sample-C):

- 1. The TGA results of Sample-A deposits (liquid hydrocarbon; inlet strainer) showed approximately 87.0 wt% of organic and 13.0 wt% of inorganic containing materials. The small quantity of the inorganic crystalline materials part of deposits obtained from XRD data and Rietveld method are consisted of mallardite, sodium iron oxide, calcium sulfate, iron sulfide.
- 2. Sample-B deposits (collected from inlet nozzles of multiple BAHEs) obtained from TGA showed that both organic and inorganic materials concentrations 11.0 wt% and 89.0% wt%, respectively. The XRD results of the inorganic crystalline materials part of deposits are consisted of iron oxide corrosion products in the form of magnetite (Fe₃O₄), calcium aluminium oxide (CaAl₂O₄), silicon oxide formation materials in the form of quartz (SiO₂) and sulfur oxide (SO₂).
- 3.TGA results of Sample-C (collected from bottom of dehydration unit dust filters) showed 14.0 wt% of organic and 86.0% of inorganic materials. The inorganic crystalline materials part of deposits consists of iron sulfide corrosion products in the

form of pyrrhotite (Fe $_{0.941}$ S); sodium aluminum silicon oxide-(Na $_2$ Al $_2$ Si $_{1.85}$ O $_{7.7}$ 5.1H $_2$ O) and silicon oxide formation materials in the form of quartz (SiO $_2$).

- 4. Moreover, GC-MS screening showed that the organic fraction of the samples (or soluble part or hydrocarbon) indicates the present of
 - Alkane C_9 - C_{25+} and elemental sulfur (S_8) in addition to triethylene glycol, methyldiethanolamine (MDEA), piperazine, 1-methyl- and other unidentified organic compounds for Sample-A.
 - Alkane C_9 - C_{25+} and elemental sulfur (S_8) in addition to butyl glycol and other unidentified organic compounds for Sample-B.
 - Alkane traces of C₉-C₂₅+ in addition to elemental sulfur (S₈), butyl glycol and other unidentified organic compounds for Sample-C.

The Sample-C showed the presence of desiccant materials (ceramic balls - Al_2O_3 and SiO_2) and it might be due the fact that the desiccant materials were crushed and escaped from the dehydration unit. It can also be seen visually in the deposited Sample-C. Also, iron sulfide corrosion products in the form of pyrrhotite (Fe0.941S) was appeared in the deposited product about 50.0%, which might be due the presence of hydrogen sulfide (H_2S) and/or elemental sulfur (S) in the system.

The observations from Amine Unit deposits are (Sample-D and Sample-E):

1. Sample-D (collected from the Amine Contactor section) showed the 26.0 wt% of organic compounds and 74.0 wt% of

inorganic compounds. The inorganic crystalline materials part of deposit is comprised of sodium calcium magnesium iron silicate ($Na_{0.64}Ca_{0.36}Mg_{0.32}Fe_{0.68}Si_2O_6$), iron sulfide corrosion products in the forms of mackinawite (FeS) and greigeite (Fe_3S_4), and iron oxide corrosion products ($Fe_{2.938}O_4$).

- 2. Sample-E (collected from the Amine Regenerator section) showed the 77.0 wt% of organic and 23.0 wt% of inorganic compounds. The 23.0 wt% of inorganic crystalline materials are consisted of calcium magnesium iron carbonate $[Ca_{0.91}Mg_{0.06}Fe_{0.03}(CO_3)]$, calcium sulfate hydrate $[Ca(SO_4)(H_2O)_2]$, silicon oxide formation materials in the form of quartz (SiO_2) ; calcium magnesium carbonate $[Ca(MgCO_3)_2]$, calcium carbide $[CaC_2]$ phases/compounds.
- 3. Moreover, GC-MS screening showed that the organic fraction of the samples (or soluble part or hydrocarbon) indicates the present of
 - Alkane traces of C₂₀ C₂₅ in addition to, Elemental Sulfur (S₈), 1,4-Dioxan-2-ol, Diethylene glycol, Triethylene glycol (TEG) and other unidentified organic compounds for Sample-D.
 - Alkane traces of C₂₀-C₂₅ in addition to, Piperazine, Methyldiethanolamine (MDEA), Triethylene glycol (TEG) and other unidentified organic compounds for Sample-E.

In amine unit, methyldiethanolamine (MDEA) and piperazine were added to remove the acid gases (H₂S & CO₂) and theses amines could be escaped from the amine unit and reaching to NGL recovery unit.

Therefore, it can be concluded that - the spectroscopy techniques results obtained from TGA, GC-MS and ESEM/EDX - as well as these accurate and reproducible X-ray crystallography (XRD data and Rietveld method) findings can guide the field engineers at the gas plant to overcome the problems of the affected equipment by drawing up the right procedures and taking preventive action to stop the generation of those particular deposits.

References

- 1. S.N. Smith, Corrosion Product Analysis in Oil and Gas Pipelines, Materials Performance, 7 (2003) 44-47.
- 2. H.S. Khanfar, H. Sitepu, A Lab Case Study of Microbiologically Influenced Corrosion and Rietveld Quantitative Phase Analysis of X-Ray Powder Diffraction Data of Deposits from Refinery. ACS Omega Journal, 6 (2021) 11822–11831.

https://doi.org/10.1021/acsomega.0c04770.

- 3. H. Sitepu, S.R. Zaidi, Application of a New Method in Identifying the Sludge Deposits from Refineries and Gas Plants: A Case of Laboratory-Based Study, International Journal of Corrosion, Vol. 2017, Article ID 9047545, 7 pages, https://doi.org/10.1155/2017/9047545.
- 4. H. Sitepu, S.R. Zaidi, Application of X-ray Powder Diffraction and Rietveld Phase Analysis to Support Investigations of Failure for Submersible Pump, Saudi Aramco Journal of Technology, Winter Edition, 2017.
- 5. H. Sitepu, Texture and Structural Refinement Using Neutron Diffraction Data from Molybdite (MoO₃) and Calcite (CaCO₃) Powders and a Ni-rich Ni50.7Ti49.30 Alloy, Powder Diffraction, 24 (2009) 315-326.

- 6. H. Sitepu, B.H. O'Connor, D.Y. Li, Comparative Evaluation of the March and Generalized Spherical Harmonic Preferred Orientation Models Using X-ray Diffraction Data for Molybdite and Calcite Powders, Journal of Applied Crystallography, 38 (2005) 158-167.
- 7. T. Degen, M. Sadki, E. Bron, U. König, et. al., The High Score Suite, Powder Diffraction, 29 (2014) S13-S18.
- 8. [1]ICDD (2018). PDF-4+ 2019 (Database), edited by Dr. Soorya Kabekkodu, International Centre for Diffraction Data, Newtown Square, PA, USA, 2018.
- 9. R.J. Hill, C.J. Howard, Quantitative Phase Analysis from Neutron Powder Diffraction Data Using the Rietveld Method, J. Appl. Cryst. 20 (1987) 467-474.
- 10. B.H. O'Connor, M.D. Raven, Application of the Rietveld Refinement Procedure in Assaying Powdered Mixtures. Powder Diff. 3 (1988) 2-6.
- 11. D.L. Bish, S.A. Howard, Quantitative Phase Analysis Using the Rietveld Method. J. Appl. Cryst. 21 (1988) 86-91.
- 12. R.J. Hill, Expanded Use of the Rietveld Method in Studies of Phase Mixtures, Powder Diff. 6 (1991) 74-77.
- 13. N.V.Y. Scarlett, I.C. Madsen, Quantification of Phases with Partial or No Known Crystal Structure, Powder Diffraction, 21 (2006) 278-284.
- 14. G. Schmitt, "Effect of Elemental Sulfur on corrosion in sour gas system," Corrosion, 47, 4 (1991) p.285.

15. S.H. Sharidi, H. Sitepu, A Laboratory-Based Case Study to Remove MTBE from Contaminated Water with Pure-WO3 and Nano-WO3 Catalysts Loaded with Ru and Pt. American Journal of Materials Synthesis and Processing, 5 (2020) 1-9. DOI: 10.11648/j.ajmsp.20200501.11.

16. D. Lianhui, H. Sitepu, S. Bogami, T. Mazin, S. Kareem, S. Essam, Effect of Zeolite-Y Modification on Crude Oil Direct Hydrocracking. American Chemical Society (ACS) Omega, 6 (2021) 28654-28662. https://doi.org/10.1021/acsomega.1c03029.

17. D.J. Pack, Elemental sulphur formation in natural gas transmission pipelines, Paper Presented at the 14th Biennal Joint Technical Meeting on Pipelines Research, Berlin, Paper No. 31, pp. 1–14, 2003.

18. J. Wang, X. Huang, W. Qi, C. Zhang, Y. Zhao, Y. Dai, T. Zhang, F. Wang, Corrosion failure analysis of the 45-degree elbow in a natural gas gathering pipeline by experimental and numerical simulation, Eng. Fail. Anal. 118 (2020) 104889.

Authors

Dr. Muthukumar Nagu is a Lead Lab scientist in the Research Analytical Services Department, Saudi Aramco. He has 23 years of experience in oilfield corrosion, including upstream, and downstream refinery, microbial corrosion, and nuclear materials. He has а Ph.D. Bharathidasan University, India, and was a postdoctoral fellow at Kyoto University, Japan. He has published 30 journal articles, 37 conferences, 2 book chapters, and holds 16 US patents. He received 20 awards including the "Best Ph.D. Award" from NACE.

Dr. Husin Sitepu is a Science Specialist in the Research Analytical Services Department (RASD), at Saudi Aramco. Dr. Sitepu is an expert in crystallography and diffraction science with а background in physics. He published 47 journal papers and presented 88 conferences. He has a Ph.D. in Physics from Curtin University. Dr. Sitepu is a member of the International Center for Diffraction Data. the International Union of Crystallography, and the Neutron Scattering Society of America.

Dr. Wala Algozeeb is a Lead Lab Scientist at Aramco's Research and Analytical Service Department, Saudi Aramco. She holds a Ph.D. from Rice University, where her research focused on the synthesis and characterization of advanced carbon materials. Dr. Algozeeb's academic background also includes an M.Sc. from the University of Manchester and a B.Sc. from Colorado State University. Her research expertise lies in tailoring carbon materials from underutilized feedstocks for highperformance applications. She published 15 journal articles and holds 5 US patents.

Dr. Nayef M Alanazi is a Research Science Consultant in the Research Analytical Services Department (RASD), Saudi Aramco, Dhahran, Saudi Arabia. Dr. Nayef has a Ph.D in materials science and engineering from Sheffield University, UK. He has 23 years of research experience in oilfield corrosion, including sour and sweet corrosion, inhibitors, coatings development, non-metallic, and materials selection. He is a member of AMPP.

Editorial **Board**

Dr. Shakeel Ahmed (Editor in Chief)

Dr. Shakeel Ahmed is a Research Scientist at the IRC for Refining & Advanced Chemicals at King Fahd University of Petroleum & Minerals. His primary areas of expertise include industrial catalysis. and instrumental inorganic synthesis, analysis. With over 200 publications and 77 co-invented patents to his name, Dr. Shakeel has made significant contributions to his field. He has been honored with numerous national and international awards and is recognized among the top 2% of scientists worldwide.

Prof. Saleh A. Ahmed

Prof. Dr. Saleh A. Ahmed received his Ph.D. in photochemistry (photochromism) under the supervision of Prof. Heinz Dürr in Saarland University. Saarbrücken. Germany. He has more than 20 years of experience as postdoctoral fellow, senior researcher and visiting professor in France, Japan, Germany, Italy and USA. Since 2010 he is currently a senior professor of organic chemistry (photochemistry) at Umm Al-Qura University/ Saudi Arabia and Assiut Egypt. He university/ successfully published more than 295 publications in high ranked journals and more than 10 USpatents. His current research interests synthesis and photophysical properties of novel organic compounds, developments of synthetic methodologies synthesis of novel organic compounds with unique theoretical and biological applications.



Dr. Faisal Alotaibi

Dr. Faisal Alotaibi, PhD in Chemical Engineering and Analytical Science from the University of Manchester, joined Saudi Aramco in 2019. He has over 17 years of experience, including roles at SABIC, KACST, and Honeywell UOP. His research focuses on zeolite synthesis, modification, and hydroconversion catalysts.

Ms. Hissah Alqahtani

Ms. Hissah Algahtani is a Lecturer in Physical Chemistry at Al Yamamah University, specializing in electrochemistry and advanced materials for energy and environmental applications. With expertise in corrosion, supercapacitors, solar cells, and water treatment, she has published extensively and holds three patents in these fields. Ms. Algahtani is also a international reviewer for scientific journals, including the Molecular Structure Journal and Springer Nature.



"Together, advancing the frontiers of chemistry for a better tomorrow "



PRINICIPAL



GOLD



STRATEGIC PARTNERS







THE JOURNAL OF CHEMICALS RESEARCH & INNOVATION SOCIETY

